Electronic Supplementary Material (ESI) for Catalysis Science & Technology.

Supporting Information

One-pot, Chemoselective Synthesis of Secondary Amines from Arylnitriles Using PdPt–Fe_3O_4 Nanoparticle Catalyst

Jin Hee Cho,[†] Sangmoon Byun,[‡] Ahra Cho,[†] and B. Moon Kim*[,†]

[†]Department of Chemistry, College of Natural Sciences, Seoul National University, 1 Gwanak-ro, Gwanak-gu, Seoul 08826, Republic of Korea

[‡]The Research Institute of Basic Sciences, Seoul National University, 1 Gwanak-ro, Gwanak-gu, Seoul, 08826, Republic of Korea

Corresponding author's email address: kimbm@snu.ac.kr

Table of Contents

page

1. Materials/Instrumentation

ESCA (Electron Spectroscopy for Chemical Analysis)

1. Model: SIGMA PROBE (ThermoVG, U.K.)
2. Condition

X-ray source		Monochromatic *Al-K* (15 kV, 100W, 400 micrometer)
Wide scan	pass energy	50 eV
	step size	1.0 eV
Narrow scan	pass energy	20 eV
	step size	0.1 eV
Flood gun	off	
Ion etching gun	off	

3. Vacuum: 7 X 10^{-9} mB (x-ray on, flood gun off)
4. Calibration: C 1s (284.5 eV)
5. Program: Avantage (ThermoVG)

Transmission Electron Microscope II (ccd camera type)

1. Model: JEM-2100
2. Accelerating Voltage: 80 to 200 kV
3. Gatan Digital Camera (ORIUS-SC600)
4. Resolution: Point image: 0.23 nm
   Lattice image: 0.14 nm
5. MAG: x50 ~ x1 500000
6. Camera Length: SA DIFF Mode: 80 ~ 2 000 mm

Cs-TEM (Cs corrected TEM with Cold FEG)

1. Model: JEM-ARM200F (Cold Field Emission Type)
2. Specifications:
   a. HT: 60, 80, 120, 200 kV
   b. Magnification: 50 to 2,000,000 X (TEM), 200 to 1,500,000 X (STEM)
   c. Resolution
      - TEM mode: Lattice 0.07 nm/ Point 0.11 nm
      - STEM mode: 0.136 nm
   d. Sample tilting
      - X / Y: ± 25° / ± 25°
3. Analysis functions:
   a. CCD Camera: UltraScan 1000XP (2,048 x 2,048 pixel)
   b. EDS: SDD Type (Active area 100 mm^2/ Solid angle 0.7 str)

Cs-STEM (Cs corrected STEM with Cold FEG)

1. Model: JEM-ARM200F (Cold Field Emission Type, JEOL)

2. Specifications
   a. HT: 60, 80, 120, 200 kV
   b. Magnification: 50 to 2,000,000 X (TEM), 200 to 1,500,000 X (STEM)
   c. Resolution
      - STEM mode: HAADF 0.1 nm/ BF 0.136 nm
      - TEM mode: Point 0.23 nm
   d. Sample tilting
      - X / Y: ±35° / ±30°

3. Analysis functions
   a. CCD Camera: UltraScan 1000XP (2,048 x 2,048 pixel)
   b. EDS: SDD Type (Active area 100 mm^2/ Solid angle 0.9 str)
   c. EELS: Model 965 GIF Quantum ER

Fe-SEM (Field Emission SEM)

1. Model: JSM-7600F (Fe-SEM)
2. Specification
   - Resolution:
      1) 1.0 nm at 15 kV
      2) 1.5 nm at 1 kV
   - Voltage range: 0.1 ~ 30 kV
   - Maximum image size: 5,120 x 3,840 pixels
   - Probe current: 1pA ~ 200 nA
   - Tilt: -5 ~ 70°
   - Rotation: 360°
   - Working Distance: 1.5 ~ 25 mm

PdPt-Fe_3O_4 samples were analyzed on Cs-STEM (Cs corrected STEM with Cold FEG), Cs-TEM (Cs corrected TEM with Cold FEG) and High resolution-Transmission Electron Microscope (ccd camera type) installed at the National Center for Inter-university Research Facilities (NCIRF) at Seoul National University.

SEM images of PdPt**–**Fe_3O_4 were obtained with a JSM-7600F at a voltage of 15 kV installed at Seoul National University Research Institute of Advanced Materials.

2. Catalyst characterization

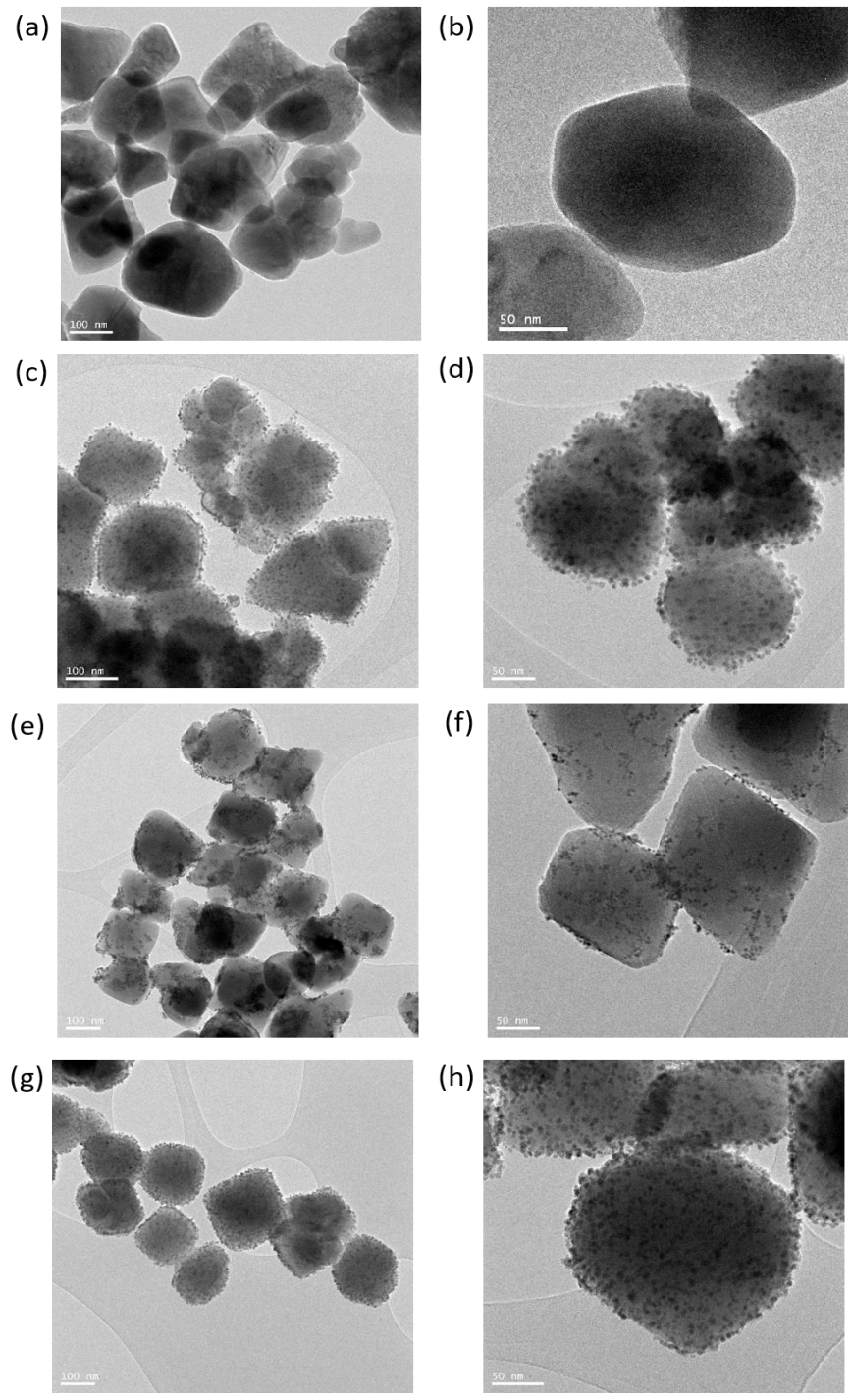

Figure S1. HR-TEM images of NPs. (a) and (b) Fe_3O_4 NPs; (c) and (d) Pd–Fe_3O_4 NPs; (e) and (f) Pt–Fe_3O_4 NPs; (g) and (h) PdPt–Fe_3O_4 NPs.

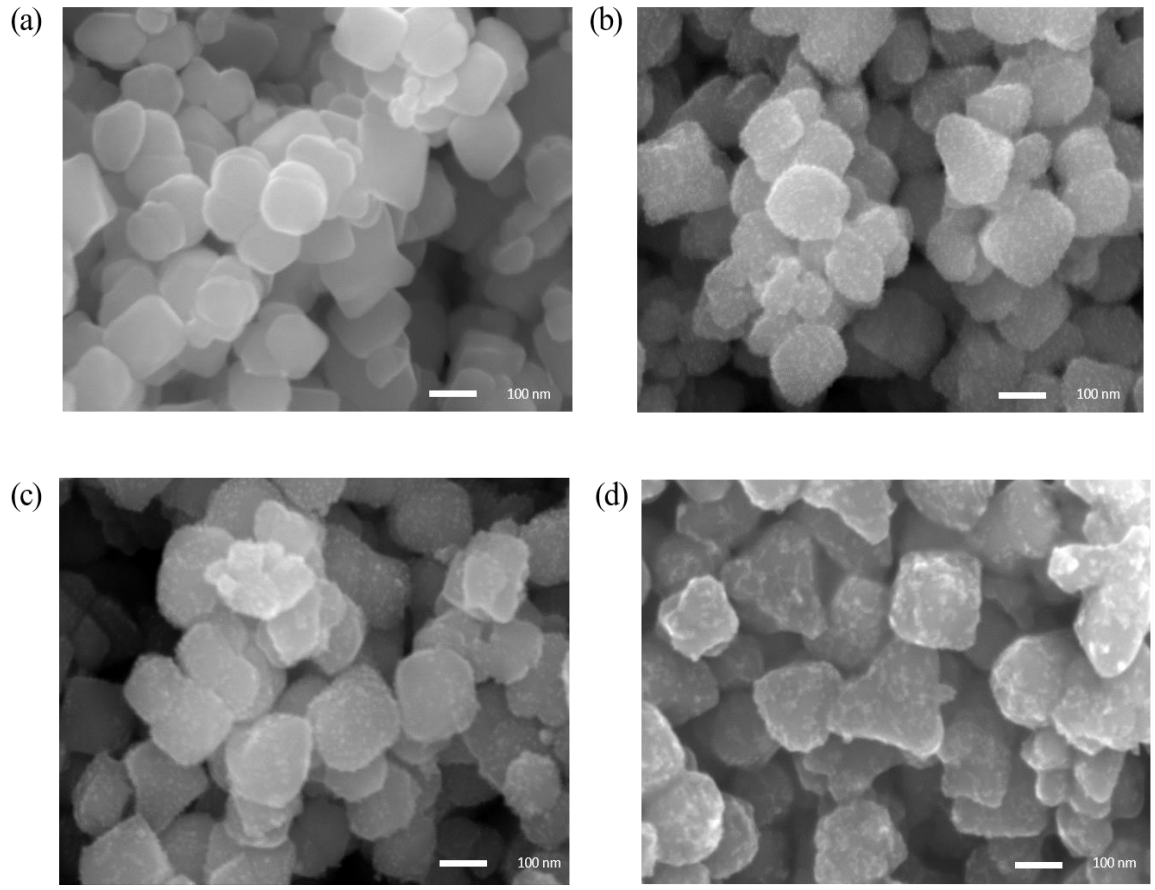

Figure S2. SEM image of (a) Fe_3O_4 NPs; (b) PdPt–Fe_3O_4 NPs; (c) Pd–Fe_3O_4 NPs; (d) Pt–Fe_3O_4 NPs.

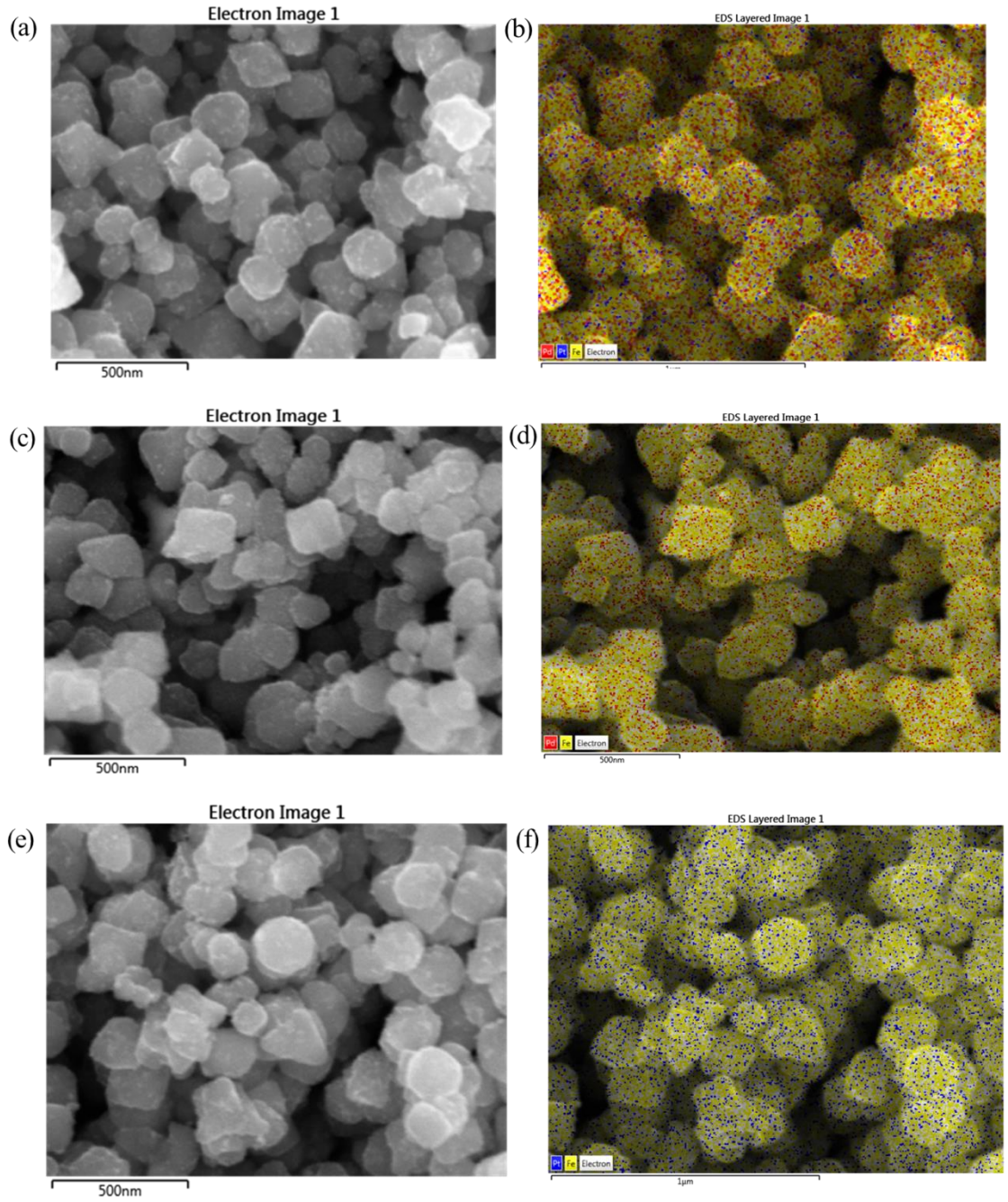

Figure S3. (a),(b) SEM-EDS images of PdPt–Fe_3O_4 NPs; (c),(d) SEM-EDS images of Pd–Fe_3O_4 NPs; (e),(f) SEM-EDS images of Pt–Fe_3O_4 NPs.

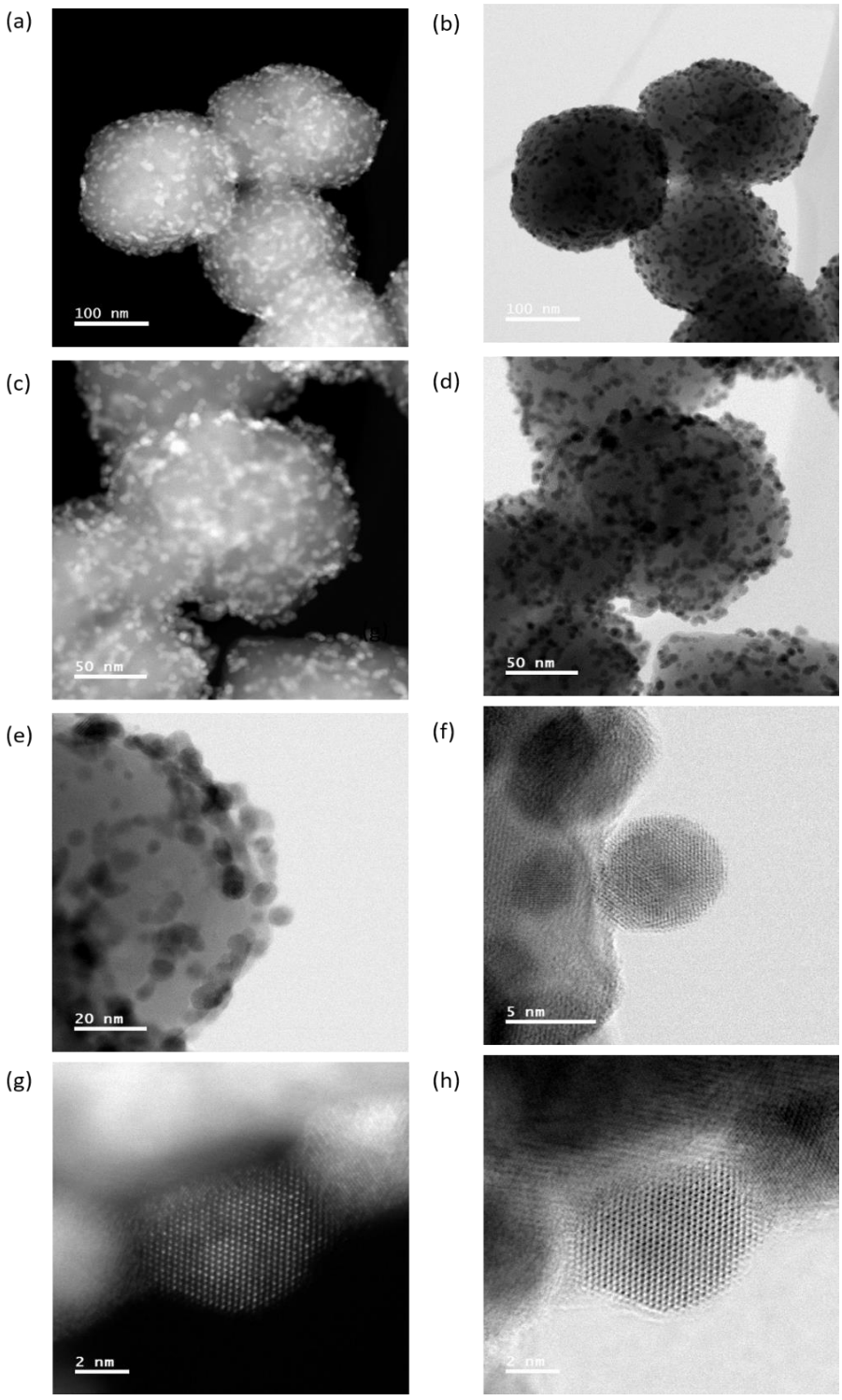

Figure S4. (a), (c), and (g) HADDF-STEM images of PdPt–Fe_3O_4 NPs; (b), (d), (e), (f), and (h) BF-STEM images of PdPt–Fe_3O_4 NPs.

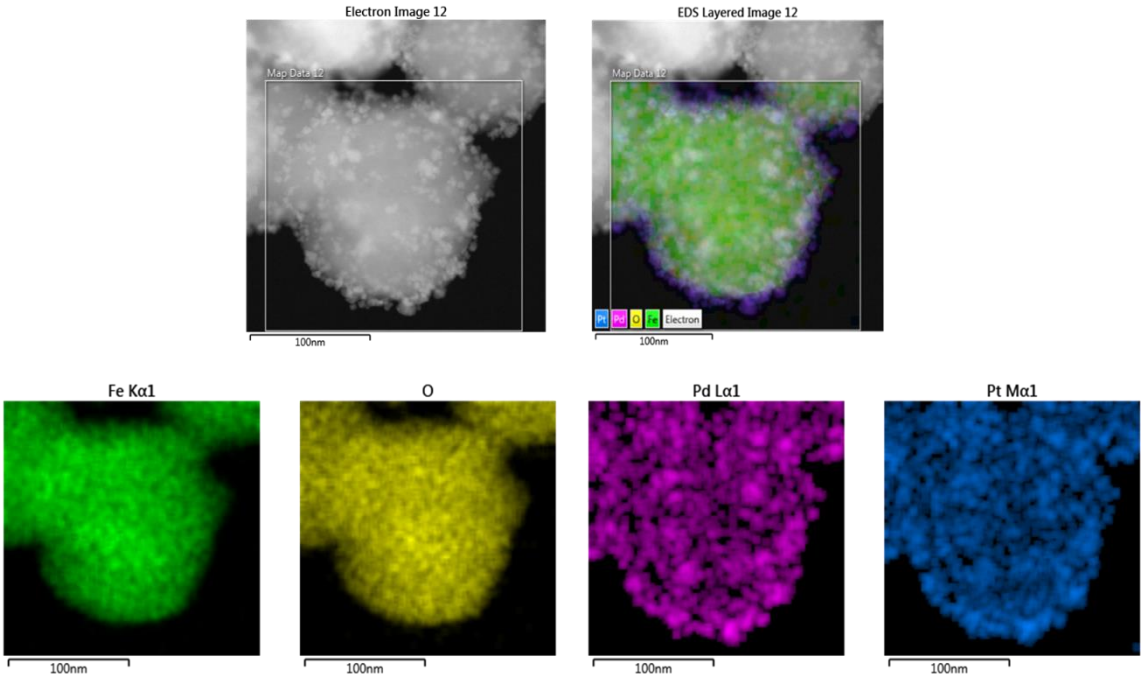

Figure S5. STEM-EDS images of PdPt–Fe_3O_4 NPs.

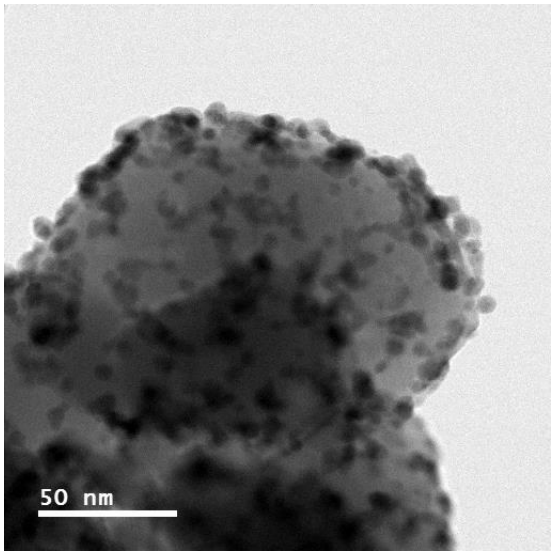

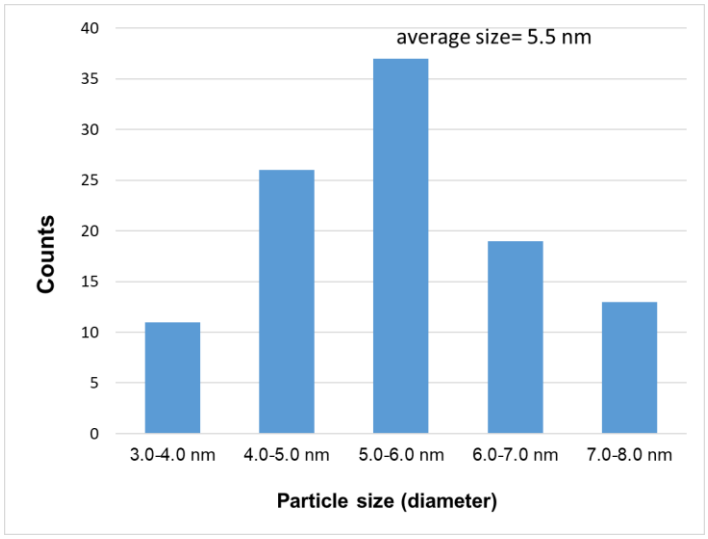

Figure S6. The particle size distribution of PdPt─Fe_3O_4 NPs.

ICP-AES Data		
Catalyst (NPs)	**Pd (wt%)**	**Pt (wt%)**
Pd–Fe_3O_4	7.47	-
Pt–Fe_3O_4	-	10.49
Fresh PdPt–Fe_3O_4	3.94	6.06
PdPt–Fe_3O_4 after 1 cycle reaction	3.87	5.91
PdPt–Fe_3O_4 after 4 cycle reaction	3.86	5.91

Figure S7. ICP-AES data of PdPt–Fe_3O_4 NPs, Pd–Fe_3O_4 and Pt–Fe_3O_4 NPs.

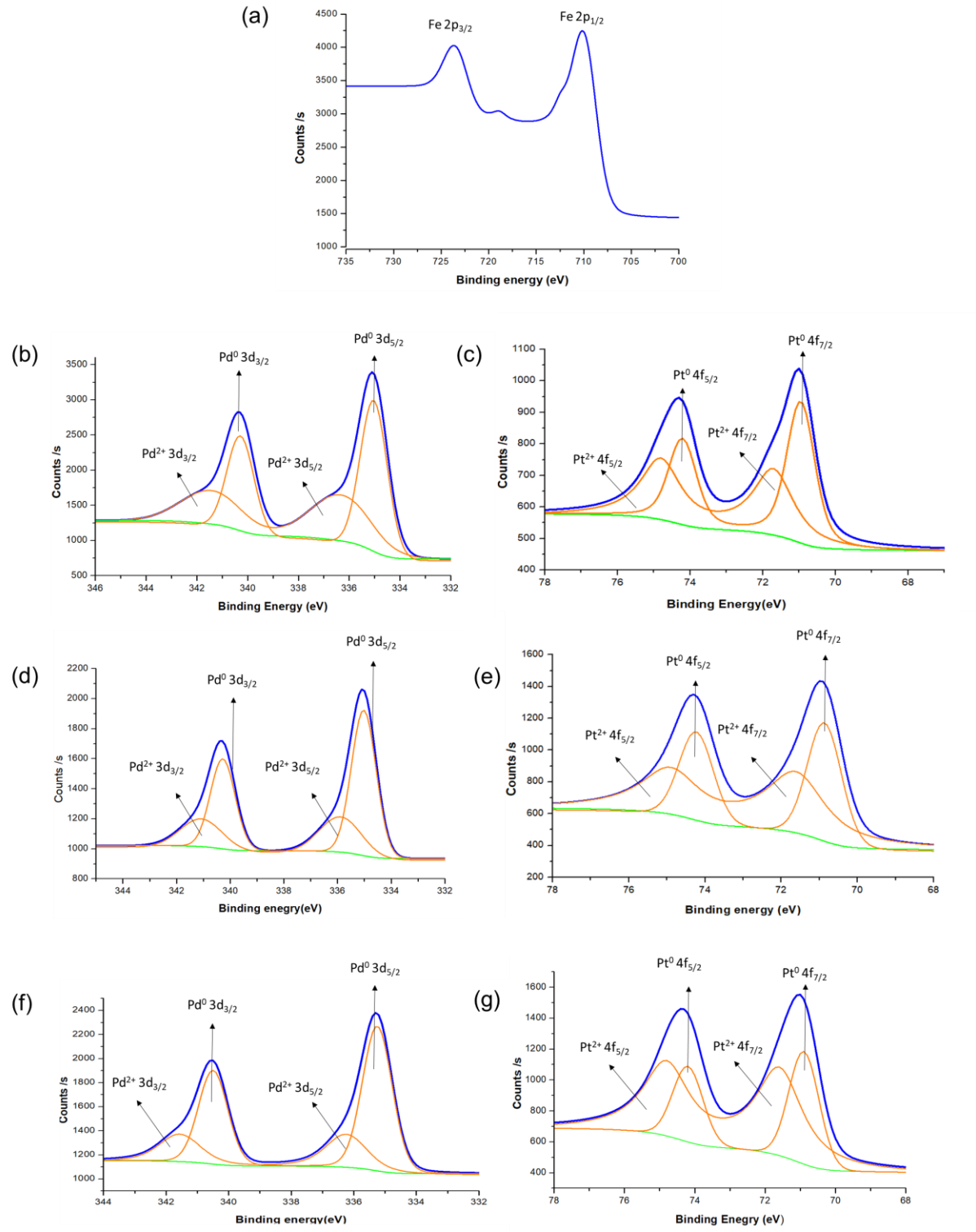

Figure S8. XPS data. (a) Fe 2p spectra of PdPt–Fe_3O_4; (b) Pd 3d spectra of Pd–Fe_3O_4; (c) Pt 4f spectra of Pt–Fe_3O_4; (d) Pd 3d spectra of fresh PdPt–Fe_3O_4; (e) Pt 4f spectra of fresh PdPt–Fe_3O_4; (f) Pd 3d spectra of PdPt–Fe_3O_4 after 1 cycle of the catalytic reaction; (g) Pt 3d spectra of PdPt–Fe_3O_4 after 1 cycle of the catalytic reaction

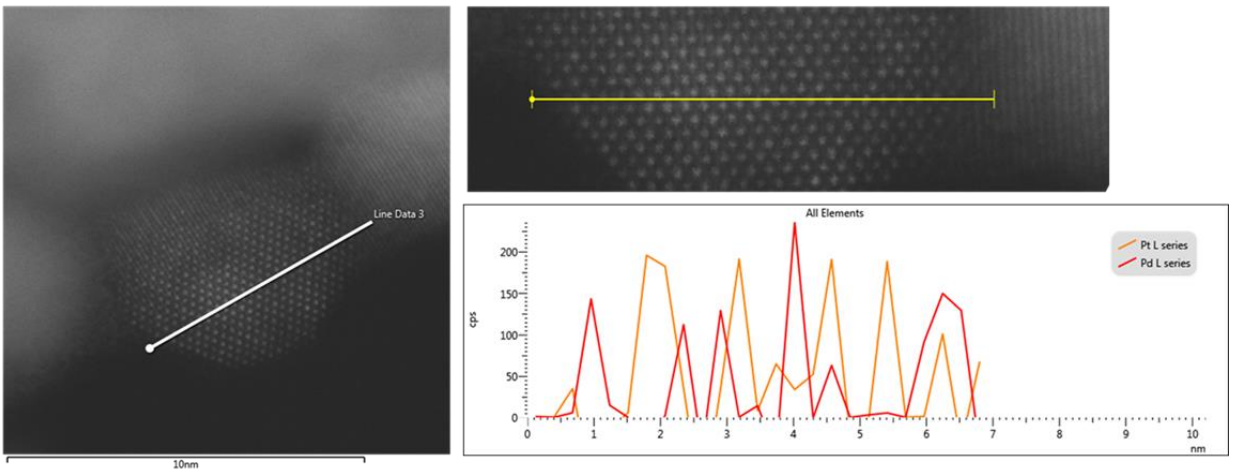

Figure S9. EDS line scan profile of a single bimetallic PdPt nanoparticle

3. Supplementary information of tables and figures.

Table S1. Optimization of the reaction condition of the hydrogenation of benzonitrile[a]

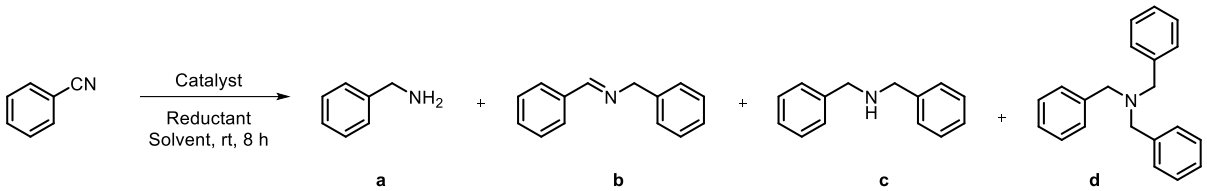

Entry	Catalyst	Reductant	Solvent	Conversion (%)	Selectivity[b] (%)			
					a	b	c	d
1	4 mol% Pd–Fe_3O_4	$NaBH_4$	MeOH	60	0	0	60	0
2	4 mol% Pt–Fe_3O_4	$NaBH_4$	MeOH	54	0	54	0	0
3	2 mol% PdPt–Fe_3O_4	NH_3BH_3	MeOH	38	0	37	1	0
4	2 mol% PdPt–Fe_3O_4	$NaBH_4$	MeOH	100	1	1	98	0
5	2 mol% PdPt–Fe_3O_4	$NaBH_4$	EtOH	81	75	5	1	0
6	2 mol% PdPt–Fe_3O_4	$NaBH_4$	i-PrOH	NR	-	-	-	-
7	2 mol% PdPt–Fe_3O_4	$NaBH_4$	Toluene	NR	-	-	-	-
8	2 mol% PdPt–Fe_3O_4	$NaBH_4$	H_2O	NR	-	-	-	-
9	2 mol% PdPt–Fe_3O_4	H_2	MeOH	NR	-	-	-	-
10	2 mol% PdPt–Fe_3O_4	$PhMe_2SiH$	MeOH	NR	-	-	-	-

[a] Reaction condition: 0.3 mmol benzonitrile, 0.6 mmol $NaBH_4$, 1.8 mL MeOH, 8 h, room temperature. [b] GC yield.

Table S2. Comparison of the catalytic activity of PdPt–Fe_3O_4 with other reported heterogeneous catalytic system for formation of dibenzylamine from benzonitrile

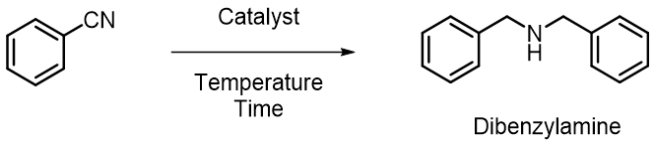

Entry	Catalyst	Reductant	Temperature	Time	Yield (%)
1[1]	Rh/AlO_3	H_2 (1 bar)	RT	20 h	85
2[2]	Pt nanowire	H_2 (4 bar)	80 °C	24 h	99
3[3]	Pd-$Fe_{0.25}Cu_{0.25}/Fe_3O_4$	NH_3BH_3	40 °C	1.5 h	98
4[4]	Pd@mpg-C_3N_4	H_2 (10 bar)	RT	6 h	89
5[5]	PtMo WNWs	H_2 (1 bar)	40 °C	24 h	91
6[6]	5NiO–Pd/SiC	H_2 (1 bar)	30 °C	5 h	98
7	PdPt–Fe_3O_4	$NaBH_4$	RT	8 h	98

Table S3. Comparison of yields with different nitrile and nitro compound stoichiometries[a]

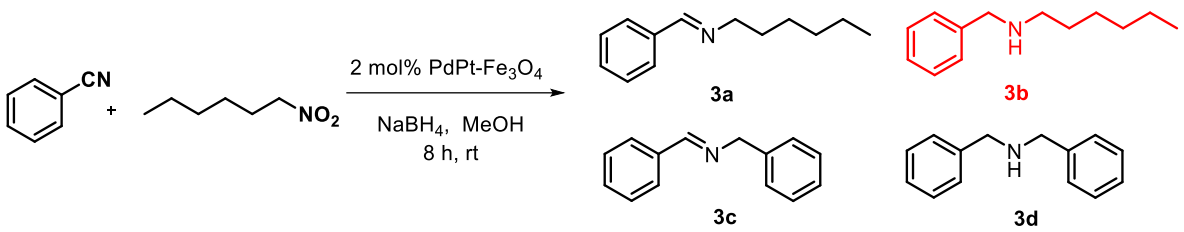

Entry	benzonitrile (equivalent)	1-nitrohexane (equivalent)	Yield[b]			
			3a (%)	**3b (%)**	**3c (%)**	**3d (%)**
1	1.5	1	0	86	0	64
2	1.2	1	0	73	5	42
3	1	1	4	62	1	27
4	1	1.2	8	72	0	20
5	1	1.5	45	50	1	4

[a] Reaction condition: 2.0 mol% PdPt–Fe_3O_4, 0.3 mmol scale, 0.6 mmol $NaBH_4$, 1.8 mL MeOH, 8 h, room temperature. [b] GC yield.

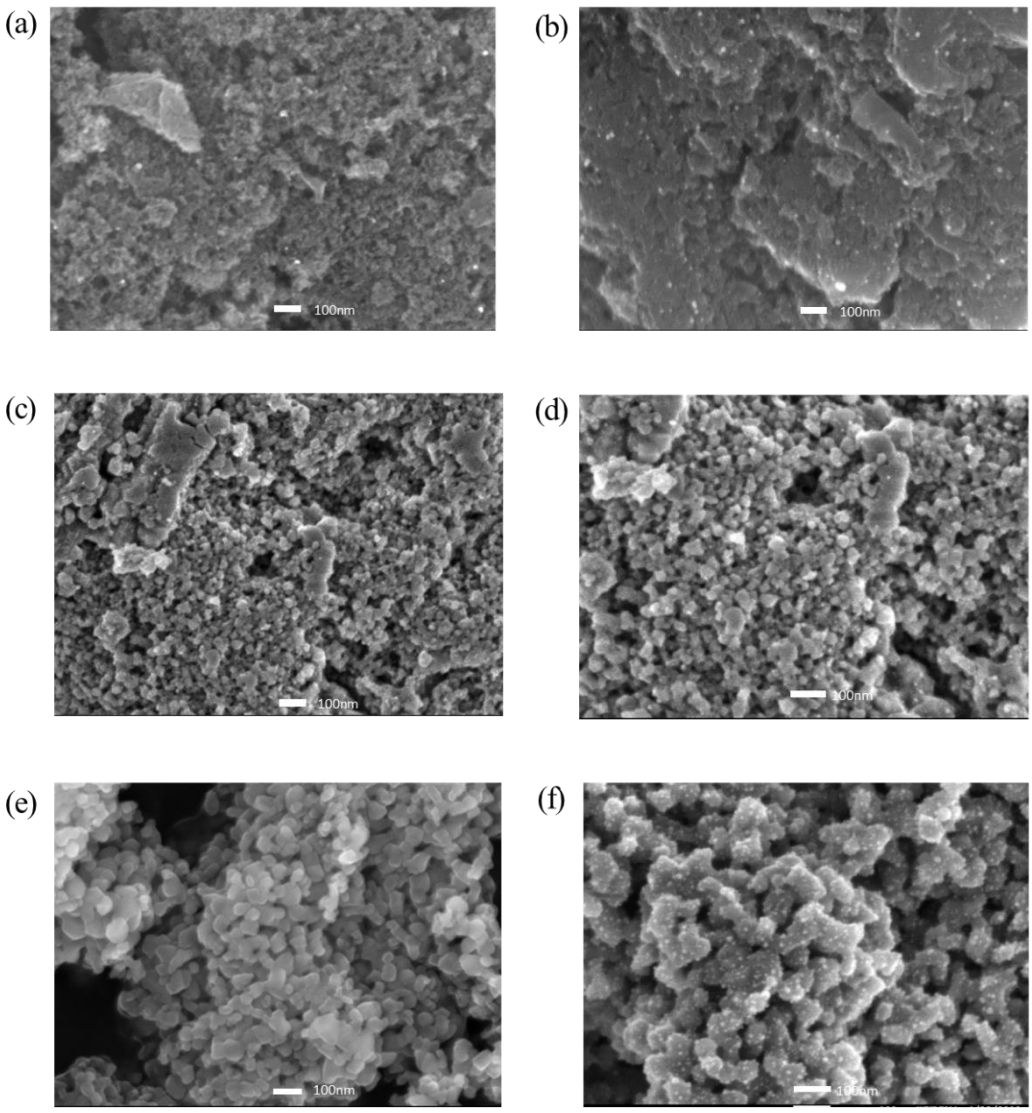

Figure S10. SEM images (a) C NPs; (b) PdPt–C NPs; (c) CeO_2 NPs; (d) PdPt–CeO_2 NPs; (e)TiO_2 NPs; (f) PdPt–TiO_2 NPs.

Catalyst	Pd (wt%)	Pt (wt%)	Pd : Pt
PdPt-C	0.94	0.84	2.05 :1
PdPt-CeO_2	2.88	4.78	1.13 : 1
PdPt-TiO_2	1.04	1.58	1.21: 1

Figure S11. ICP-AES data of PdPt NPs with different supports.

(a)

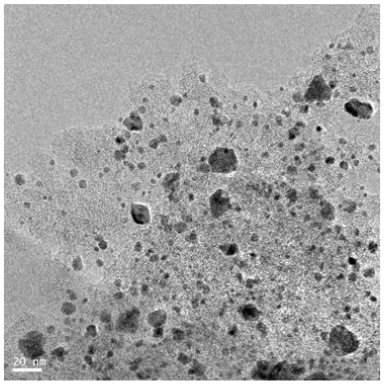

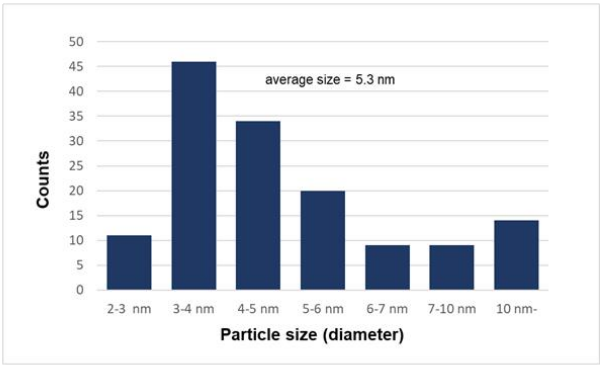

PdPt-C

(b)

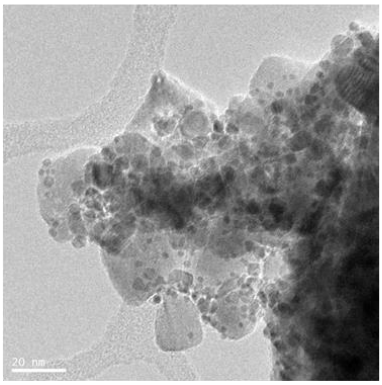

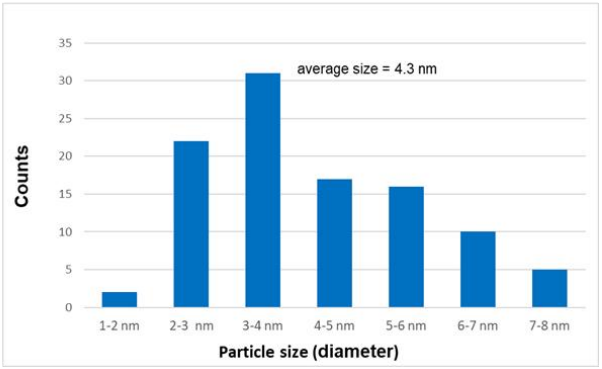

PdPt-CeO_2

(c)

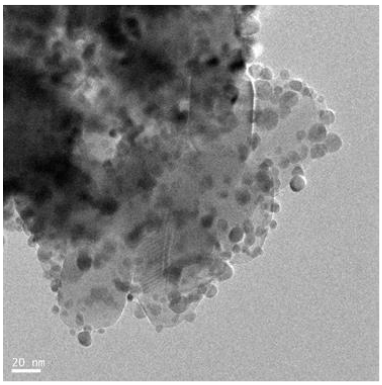

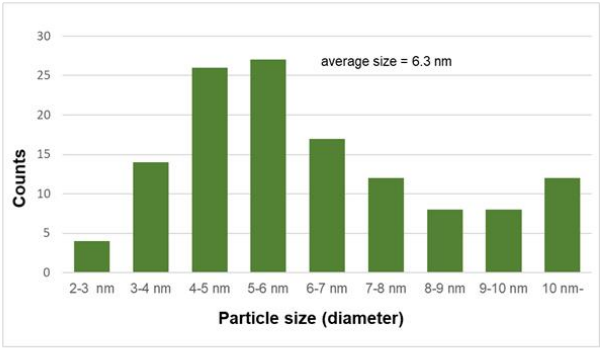

PdPt-TiO_2

Figure S12. The particle size distribution. (a) PdPt–C NPs; (b)PdPt–CeO_2 NPs; (c) PdPt–TiO_2 NPs.

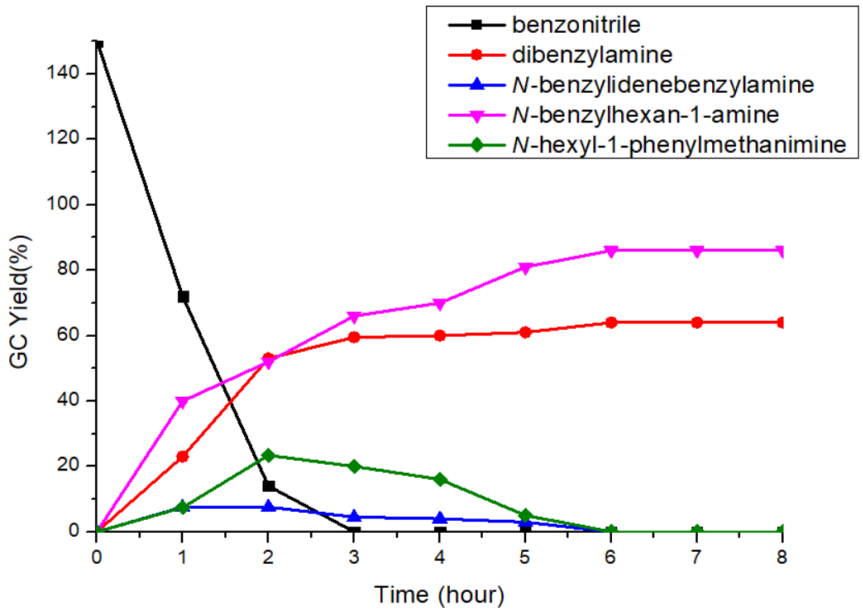

Reaction condition: 2.0 mol% catalyst, 0.45 mmol of benzonitrile, 0.30 mmol of 1-nitrohexane, 0.60 mmol $NaBH_4$, 1.8 mL MeOH, 8 h, room temperature.

Figure S13. Conversion versus time plot for *N*-benzylhexan-1-amine formation from the reductive amination of benzonitrile with 1-nitrohexane using PdPt–Fe_3O_4 NPs catalyst.

(a) 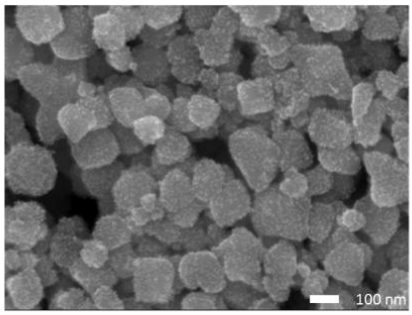

(b) 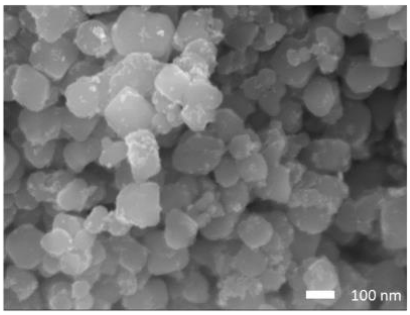

(c)

Catalyst	Pd (wt%)	Pt (wt%)	Molar ratio
$Pd_{2.3}Pt_1$-Fe_3O_4	7.57	6.16	2.3:1
$Pd_1Pt_{0.97}$-Fe_3O_4	3.81	6.85	1:0.97
$Pd_1Pt_{1.7}$-Fe_3O_4	3.00	9.52	1:1.7

Figure S14. (a) SEM image of $Pd_{2.3}Pd_1$–Fe_3O_4 NPs; (b) SEM image of $Pd_1Pd_{1.7}$–Fe_3O_4 NPs; (c) ICP-AES data of Pd_xPd_y–Fe_3O_4 NPs.

Table S4. Comparison catalytic activity of Pd_xPd_y–Fe_3O_4 NPs for the unsymmetrical amine under the optimized condition[a]

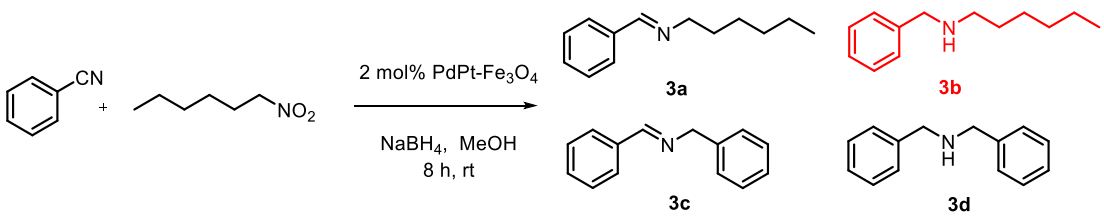

Catalyst	Benzonitrile (Conversion; 150%)	Yield (%)	Selectivity[b]				TON (Turnover number)
			3a (%)	3b (%)	3c (%)	3d (%)	
Pd–Fe_3O_4	40	27	0	27	0	10	13
$Pd_{2.3}Pt_1$–Fe_3O_4	150	78	1	78	1	70	39
$Pd_1Pt_{0.97}$–Fe_3O_4	150	86	1	86	1	62	43
$Pd_1Pt_{1.7}$–Fe_3O_4	68	0	55	0	13	0	-
Pt–Fe_3O_4	25	0	23	0	1	0	-

[a] Reaction condition: 2.0 mol% catalyst (total metal contents is 4 mol%), 0.45 mmol benzonitrile, 0.30 mmol 1-nitrohexane, 0.60 mmol $NaBH_4$, 1.8 mL MeOH, 8 h, room temperature. [b] GC yield

Table S5. Additive screenings toward the reductive amination of 4-methoxybenzonitrile with 1-nitropropane for unsymmetrical secondary amine[a]

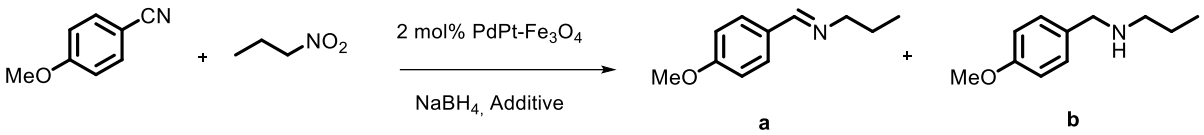

Entry	Additive (1eq)	Selectivity[b]	
		a (%)	b (%)
1	none	60	0
2	Acetic acid	37	0
3	NH_4OAc	51	0
4	NH_4Cl	65	0
5	TFE (2,2,2-Trifluoroethanol)	77	0
6	HFIP	61	2
7	$ZnCl_2$	-	-

[a] Reaction condition: 2.0 mol% PdPt–Fe_3O_4, 0.45 mmol 4-methoxybenzonitrile, 0.30 mmol 1-nitropropane, 0.90 mmol $NaBH_4$, 0.30 mmol additive, 1.8 mL MeOH, 24 h, room temperature. [b] GC yield.

Table S6. Effect of HFIP co-solvent toward the reductive amination of 4-methoxybenzonitrile 1-nitropropane for unsymmetrical secondary amine[a]

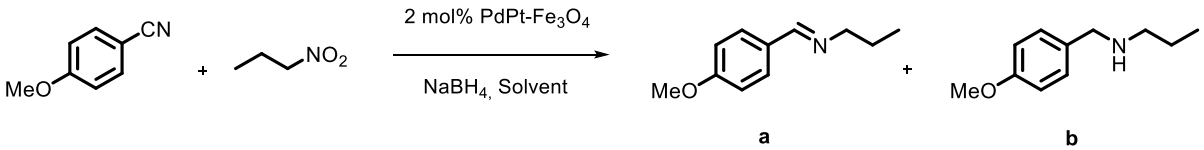

Entry	Solvent	Yield[b]	
	MeOH : HFIP ratio	**a** (%)	**b** (%)
1	MeOH only	60	0
2	1 : 1	0	91
3	2 : 1	0	92
4	4 : 1	25	53
5	5 : 1	22	35
6	10 : 1	34	0
7	HFIP only	0	56

[a] Reaction condition: 2.0 mol% PdPt–Fe_3O_4, 0.45 mmol 4-methoxybenzonitrile, 0.30 mmol 1-nitropropane, 0.90 mmol $NaBH_4$, 1.8 mL of solvent, 24 h, room temperature. [b] GC yield.

Table S7. Comparison of yields with different nitrile and amine compound stoichiometries[a]

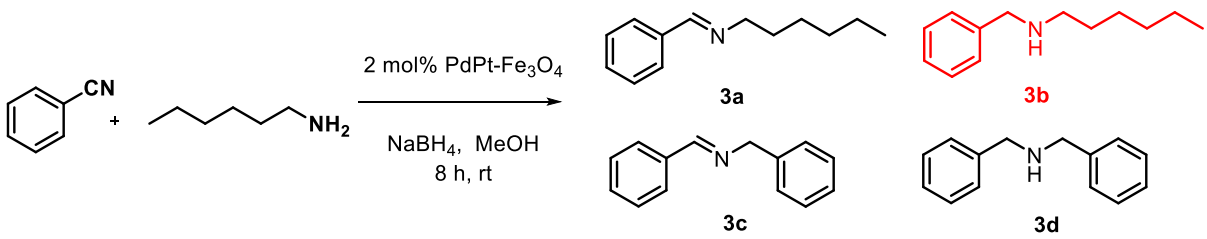

Entry	benzonitrile (equivalent)	1-hexylamine (equivalent)	Yield[b]			
			3a (%)	**3b (%)**	**3c (%)**	**3d (%)**
1	1.5	1	0	78	0	70
2	1.2	1	0	61	0	56
3	1	1	0	65	0	35
4	1	1.2	0	82	0	18
5	1	1.5	0	90	0	10

[a] Reaction condition: 2.0 mol% PdPt–Fe_3O_4, 0.3 mmol scale, 0.6 mmol $NaBH_4$, 1.8 mL MeOH, 8 h, room temperature. [b] GC yield.

Table S8. Comparison of the synthesis of unsymmetrical secondary amines from aryl nitriles using the PdPt–Fe_3O_4 catalyst with those using other heterogeneous catalytic systems.

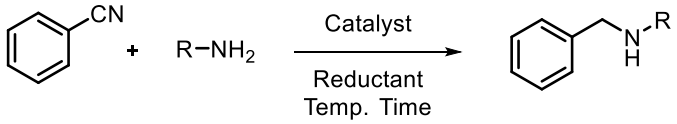

Entry	**R-**	**Catalyst**	**Reductant**	**Temp.**	**Time**	**Yield**
1[7]	Phenyl	Pd/C	H_2 (ballon)	rt	48 h	-
2[2]	Pentyl	Pt nanowire	1 bar of H_2 pressure (10 h) and 4 bars of H_2 pressure (10 h)	80 °C	20 h	93%
3[8]	Hexyl	Pt/C	6 bar of H_2	105 °C	Flow rate of liquid (0.1 mL min^{-1})	91%
4	Hexyl	PdPt-Fe_3O_4	$NaBH_4$	rt	8 h	90%[a] (80%[b])

[a] GC yield. [b] Isolated yield.

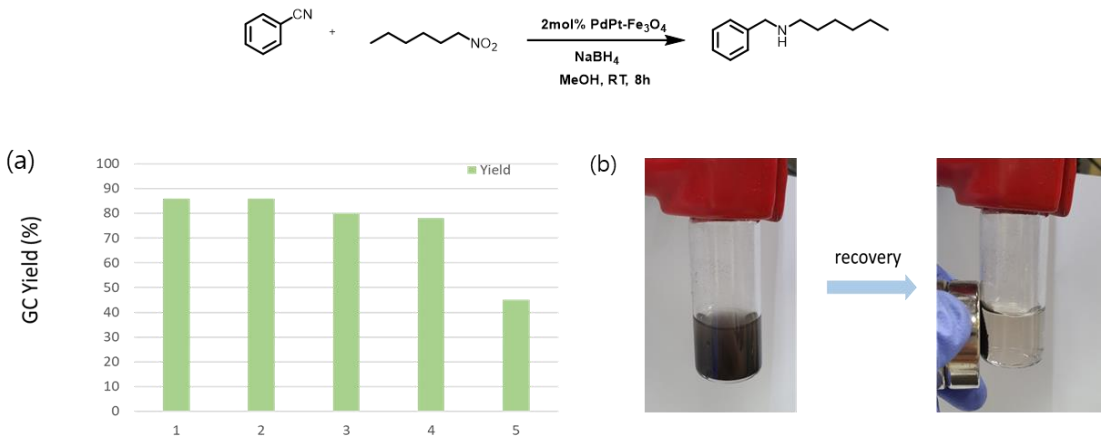

Figure S15. (a) Recyclability of PdPt–Fe_3O_4 for reductive amination of benzonitrile with 1-nitrohexane; (b) Recovery of catalyst using an external magnet.*

* Especially, when the fifth reaction was carried out, unlike the previous results, a mixture of *N*-benzylhexan-1-amine and *N*-hexyl-1-phenylmethanimine was produced. This indicates that as the reaction was repeated, the catalytic activity towards the imine reduction decreased significantly. We compared the HR-TEM images of both fresh and recovered catalysts (Figure S16). The HR-TEM image of the catalyst after 4th run showed considerable agglomeration of the PdPt nanoparticles compared to that of the fresh catalyst. To investigate the oxidation state change, we compared XPS data before and after the reaction (Figure S8) and found no change in the oxidation state. Also, ICP-AES confirmed that the Pd and Pt contents of the PdPt–Fe_3O_4 NPs from the 4th recycle had decreased only by 0.08 wt% and 0.15 wt%, respectively (Figure S7). Since the detachment of PdPt NPs was negligible, it can be confirmed that the catalyst activity was reduced due to the agglomeration of the PdPt nanoparticles, not from the catalyst detachment.

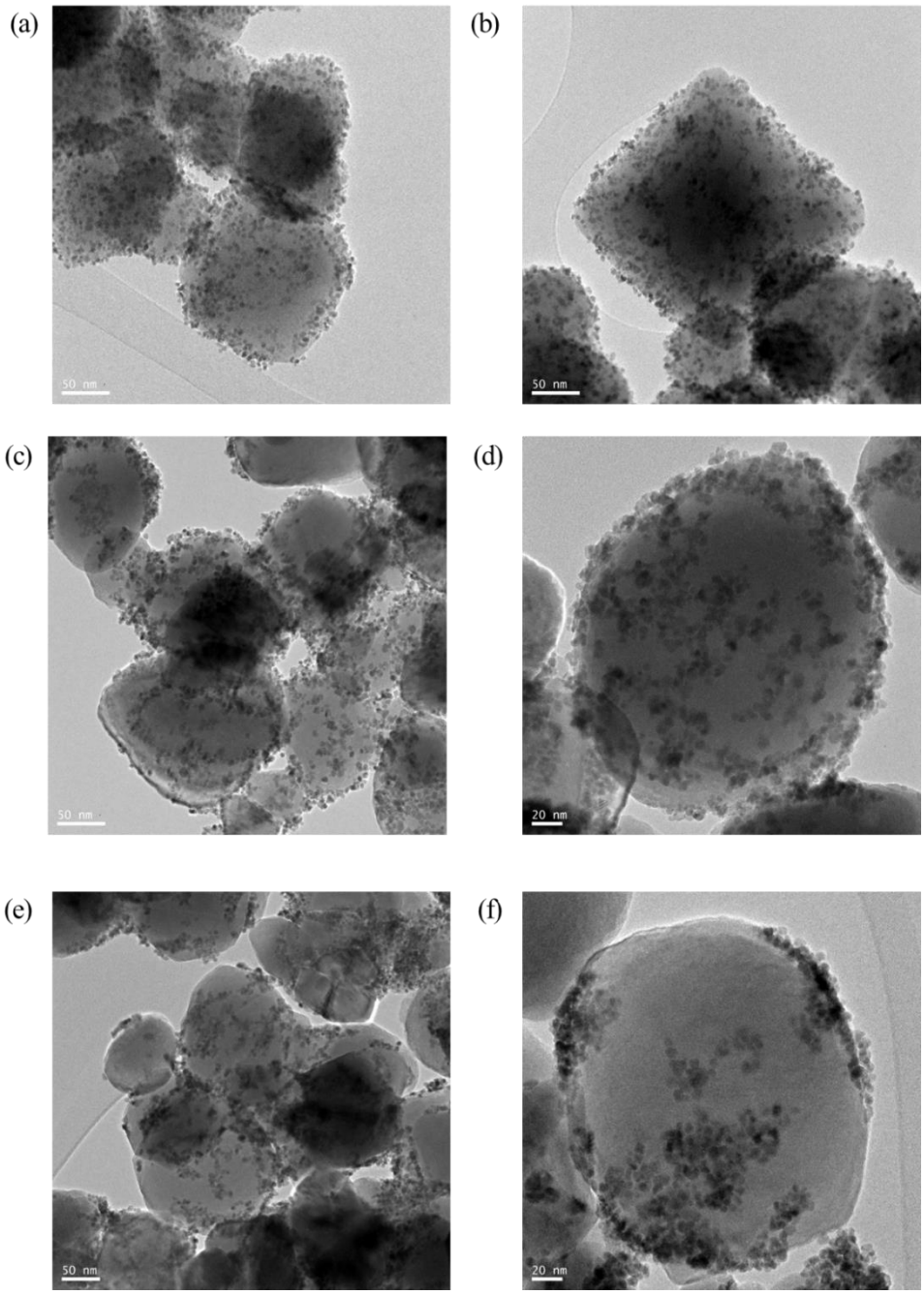

Figure S16. HR-TEM images of NPs. (a) and (b) fresh PdPt–Fe_3O_4 NPs; (c) and (d) PdPt–Fe_3O_4 NPs after 1 catalytic cycle; (e) and (f) PdPt–Fe_3O_4 NPs after 4 catalytic cycle.

4. NMR spectra

NMR S1, 3a, *N*-benzylhexan-1-amine[9]

80%(153 mg, Yellow oil);^{1}H NMR (400 MHz, $CDCl_3$) δ 7.32 (d, *J* = 4.4 Hz, 5H), 3.79 (s, 2H), 2.66 – 2.60 (m, 2H), 1.55 (br, 1H) 1.53 – 1.48 (m, 2H), 1.34 –1.24 (m, 6H), 0.88 (t, *J* = 6.7 Hz, 3H).^{13}C NMR ($CDCl_3$, 101 MHz) δ: 140.3, 128.3, 128.1, 126.8, 54.0, 49.4, 31.7, 29.9, 27.0, 22.6, 14.0

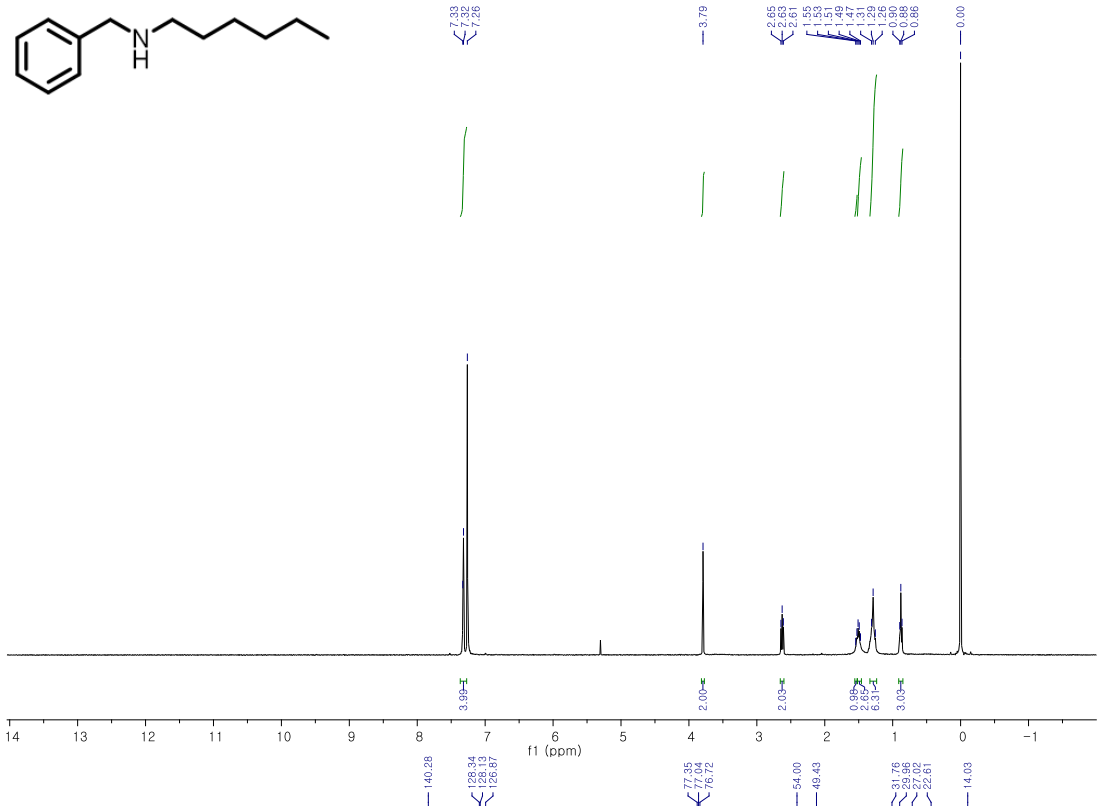

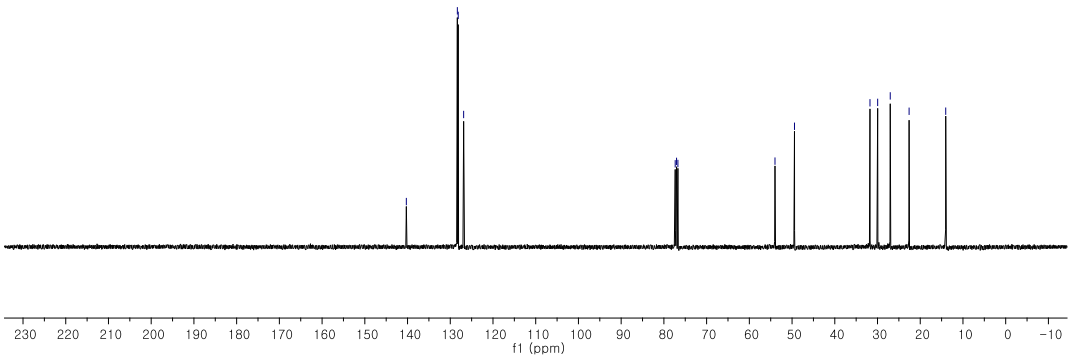

NMR S2, 3g, *N*-benzylpropan-1-amine[10]

75% (111 mg, Colorless oil) ; ^{1}H NMR (400 MHz, $CDCl_3$) δ 7.36 – 7.21 (m, 5H), 3.79 (s, 2H), 2.61 (t, *J* = 7.2 Hz, 2H), 1.59 – 1.54 (br, 1H), 1.54 – 1.48 (m, 2H), 0.92 (t, *J* = 7.4 Hz, 3H). ^{13}C NMR ($CDCl_3$, 101 MHz) δ: 140.2, 128.3, 128.2, 127.0, 53.9, 51.2, 23.0, 11.7

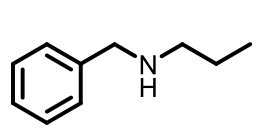

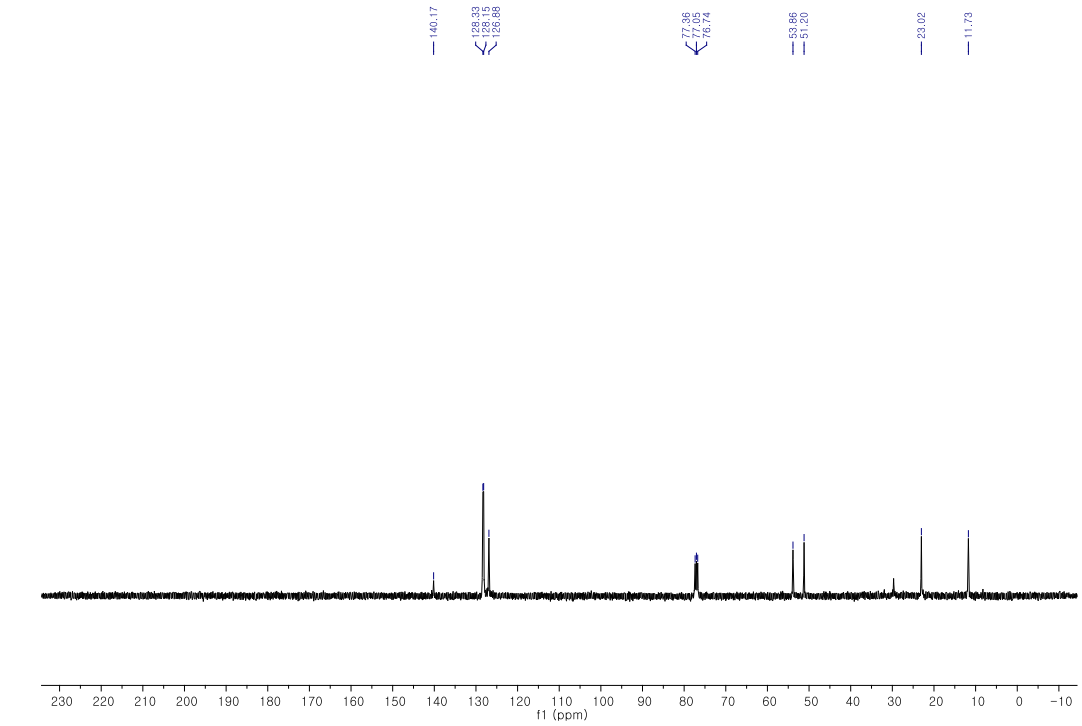

NMR S3, 3f , *N*-butylbenzylamine[11]

76% (124mg, Yellow oil); ^{1}H NMR (400 MHz, $CDCl_3$) δ 7.38 – 7.21 (m, 5H), 3.80 (s, 2H), 2.68 – 2.60 (m, 2H), 1.53-1.48 (m, 2H), 1.38-1.32 (m, 2H), 0.91 (t, *J* = 7.3 Hz, 3H). ^{13}C NMR ($CDCl_3$, 101 MHz) δ: 140.0, 128.4, 128.2, 126.9, 53.9, 49.0, 32.0, 20.5, 14.0.

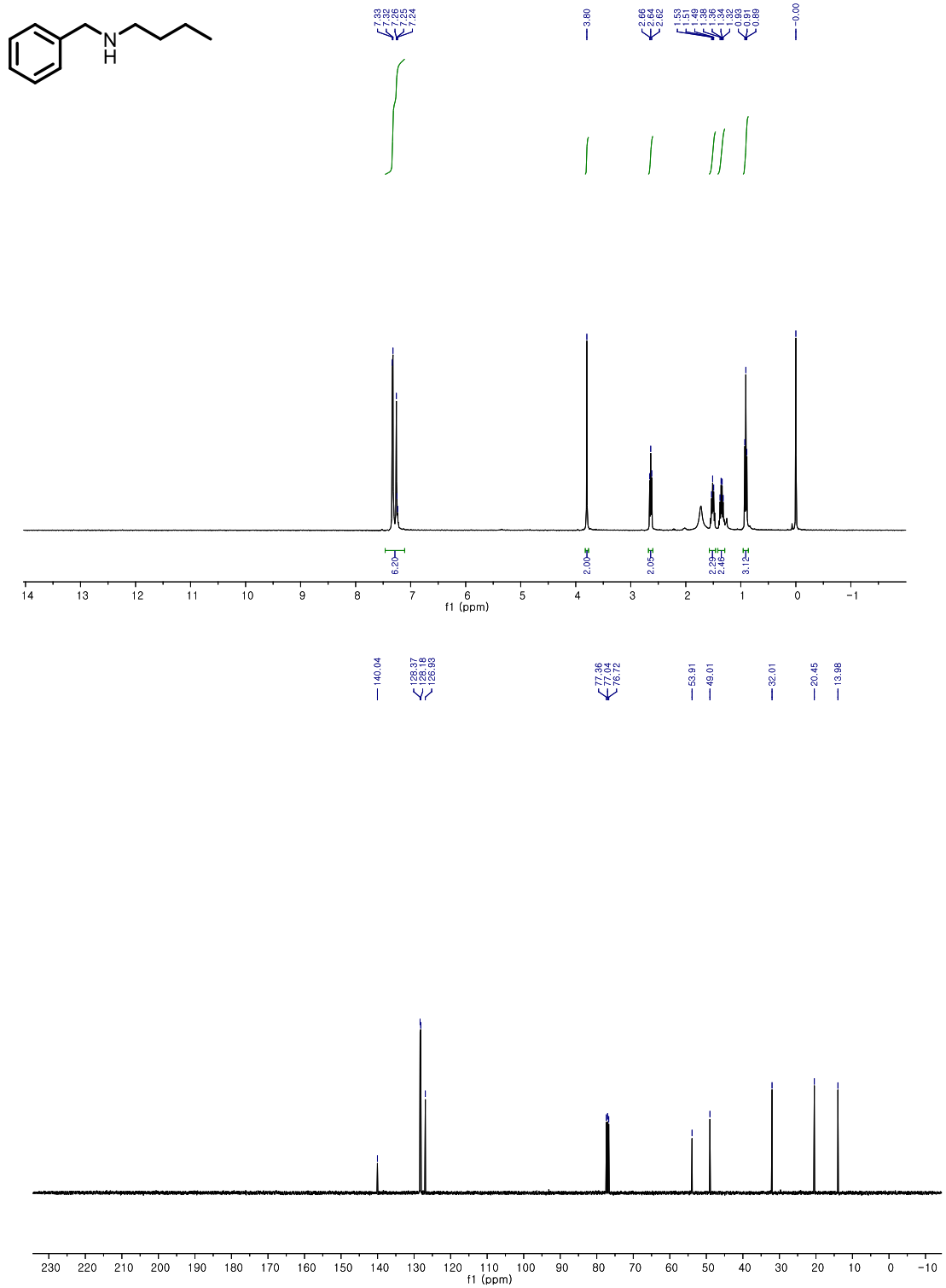

NMR S4, 3e, *N*-benzylpentan-1-amine[12]

86% (152mg, Colorless oil) ; ^{1}H NMR (400 MHz, $CDCl_3$) δ 7.32-7.23 (m, 5H), 3.79 (s, 2H), 2.63 (t, *J* = 7.3 Hz, 2H), 1.55 – 1.48 (m, 2H), 1.38 – 1.26 (m, 4H), 0.89 (t, *J* = 6.9 Hz, 3H).^{13}C NMR (101 MHz, $CDCl_3$) δ 140.4, 128.3, 128.1, 126.9, 54.0, 49.4, 29.8, 29.5, 22.6, 14.0.

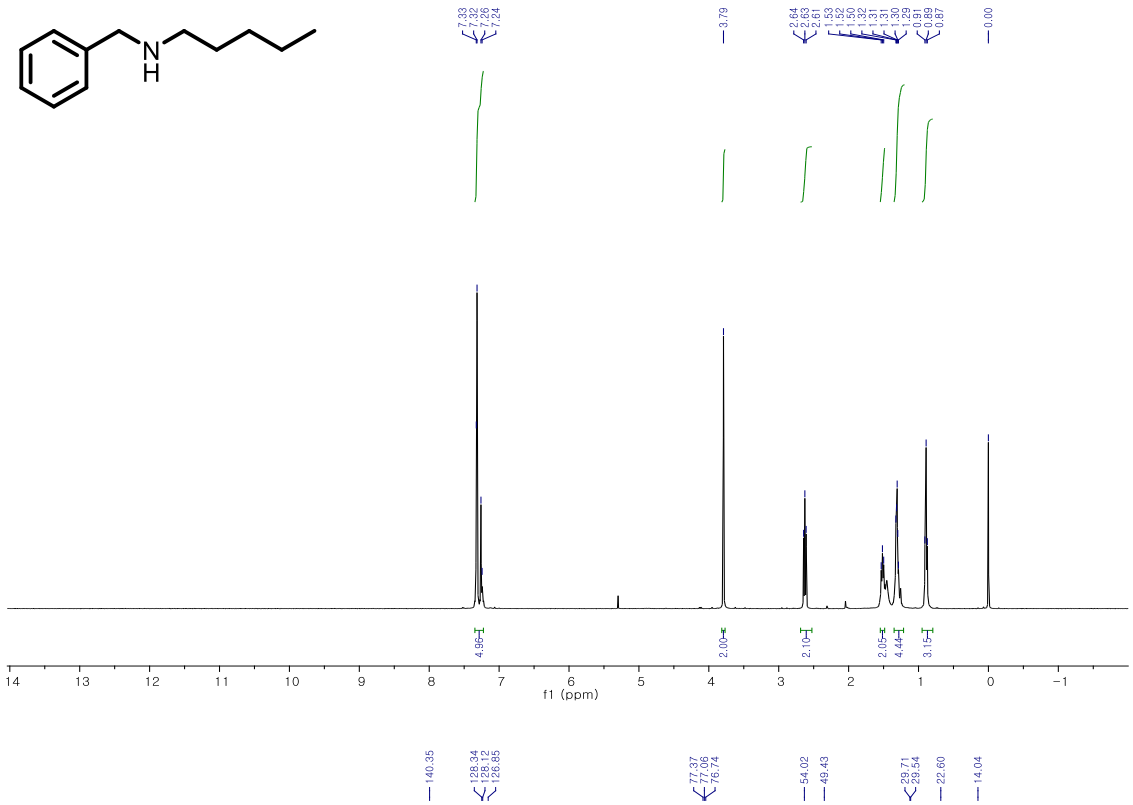

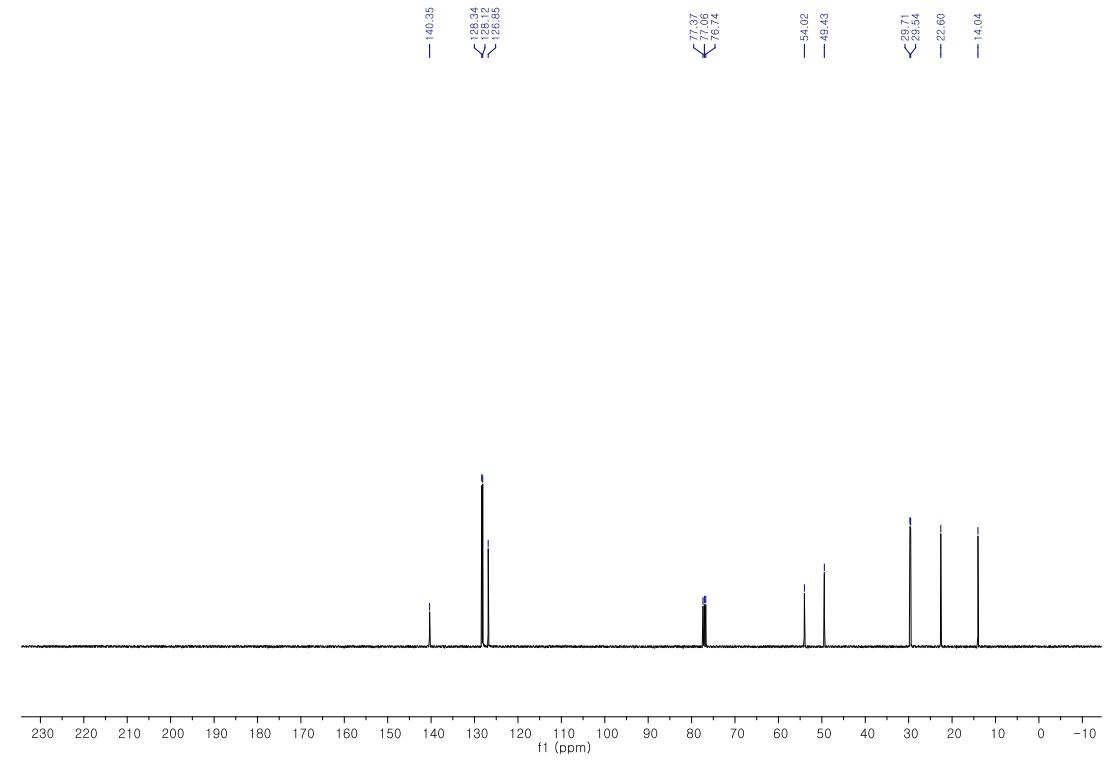

NMR S5, 3h, *N*-Benzyl-cyclopentyl-amine[13]

80% (140 mg, Yellow oil); ^{1}H NMR (400 MHz, $CDCl_3$) δ 7.35 – 7.23 (m, 5H), 3.78 (s, 2H), 3.16 – 3.07 (m, 1H), 1.91 – 1.81 (m, 2H), 1.74 – 1.66 (m, 2H), 1.57 – 1.50 (m, 2H), 1.45 – 1.35 (m, 2H). ^{13}C NMR (101 MHz, $CDCl_3$) δ 140.4,128.4,128.2,126.9, 59.1, 52.7, 33.1, 24.1.

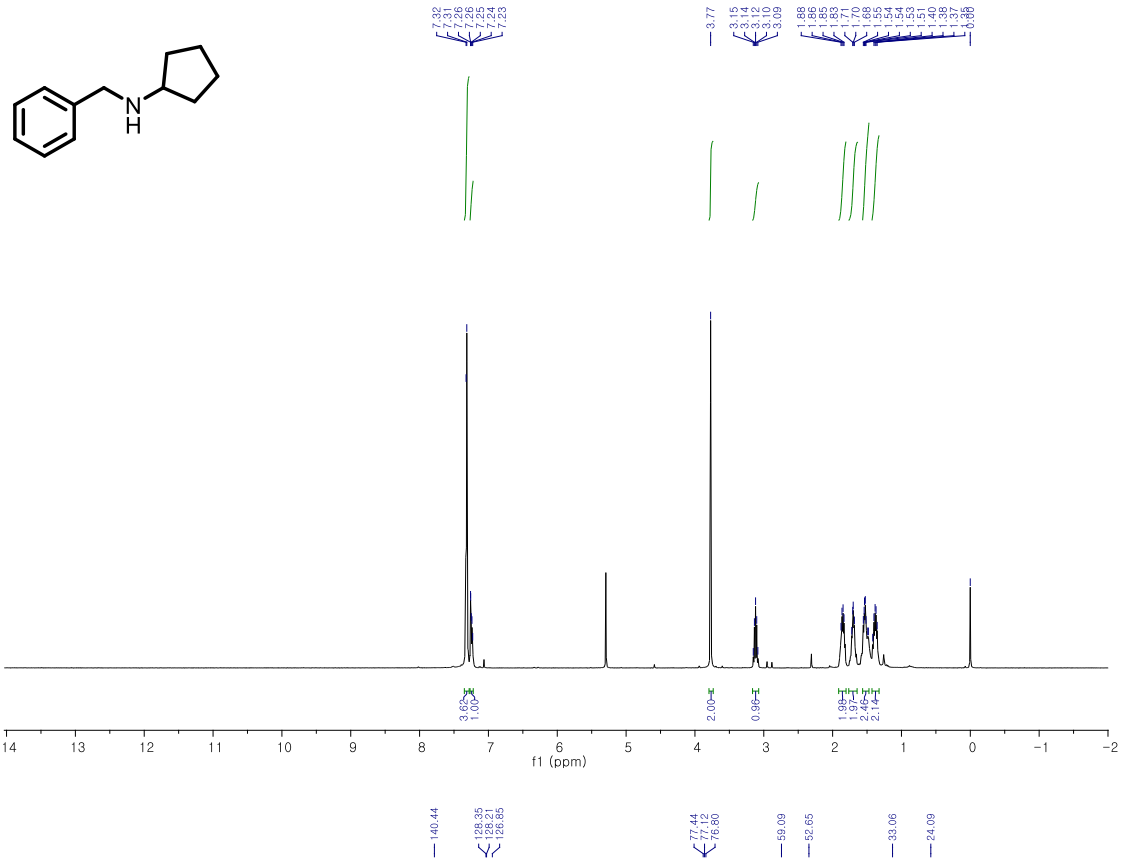

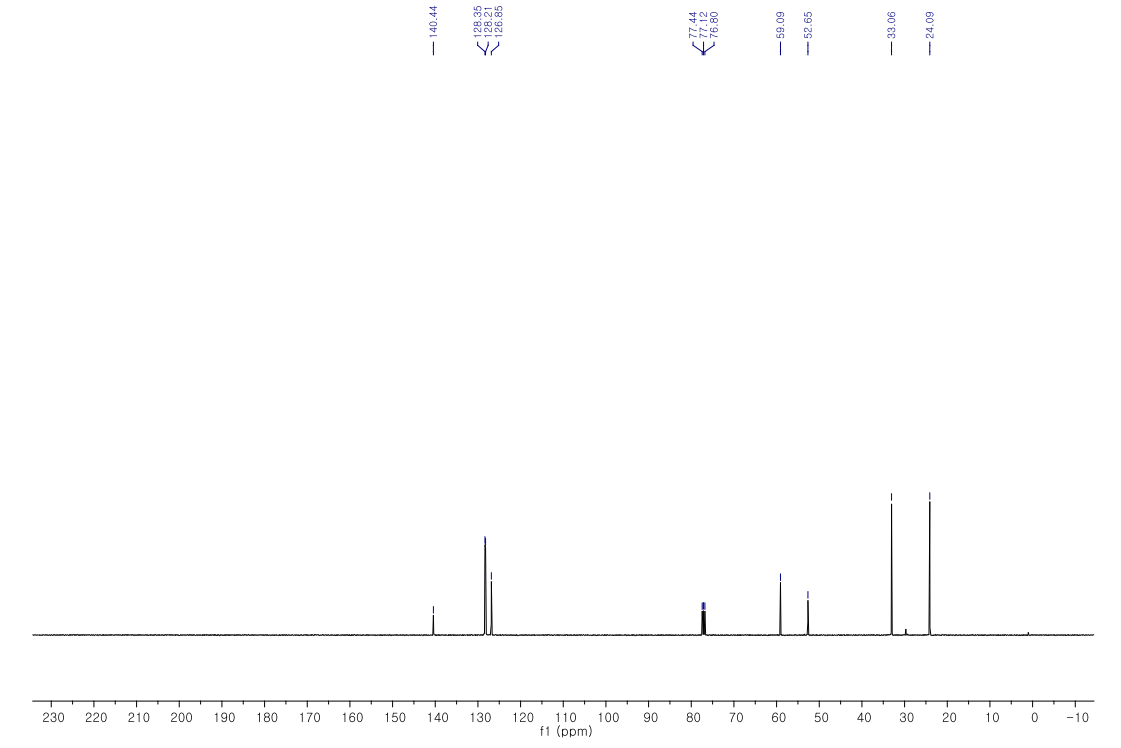

NMR S6, 3i, *N*-(3-methylbenzyl)hexan-1-amine

84% (172 mg, Yellow oil) ; ^{1}H NMR (400 MHz, $CDCl_3$) δ 7.21 (t, *J* = 7.5 Hz, 1H), 7.14 (s, 1H), 7.11 (d, *J* = 7.6 Hz, 1H), 7.06 (d, *J* = 7.4 Hz, 1H), 3.75 (s, 2H), 2.68 – 2.58 (m, 2H), 2.35 (s, 3H), 1.54 – 1.48 (m, 2H), 1.28 (t, *J* = 11.0 Hz, 6H), 0.88 (t, *J* = 6.7 Hz, 3H). ^{13}C NMR (101 MHz, $CDCl_3$) δ 140.3, 137.9, 128.9, 128.2, 127.6, 125.1, 54.0, 49.5, 31.8, 30.0, 27.0, 22.6, 21.4, 21.3, 14.0. HR-MS (EI): calcd for $C_{14}H_{23}N$ 205.1890; found: 233.1831.

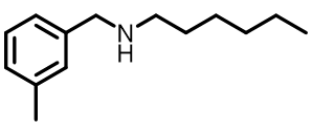

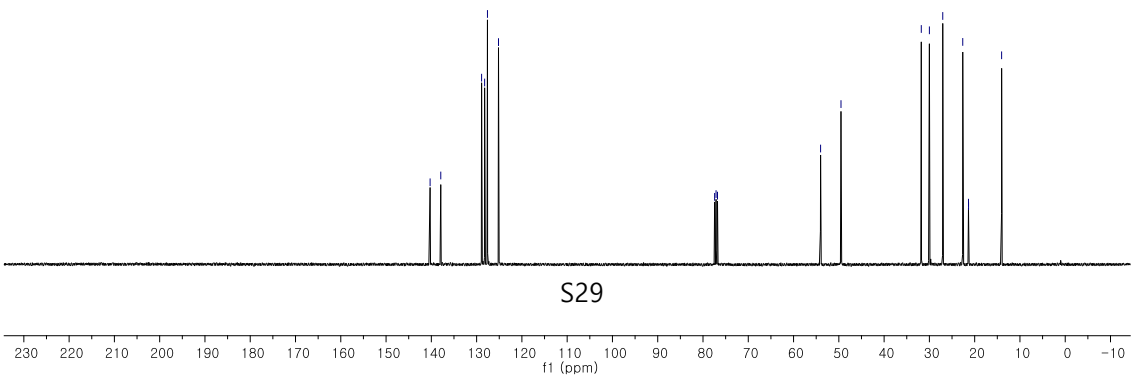

NMR S7, 3j, *N*-(4-methylbenzyl)hexan-1-amine[14]

80% (164 mg, Colorless oil); ^{1}H-NMR (400 MHz, $CDCl_3$ 1H NMR (400 MHz, $CDCl_3$) δ 7.23-21 (d, 2H), 7.14-13 (d, 2 H), 3.76 (s, 2 H), 2.62 (t, 2H), 2.33(s, 3H),1.53-1.51(m, 2H), 1.30-1.26 (m, 6H), 0.87 (t, 3H). ^{13}C NMR (101 MHz, $CDCl_3$) δ 136.7, 136.6, 129.0, 128.2, 53.5, 49.2, 31.7, 29.7, 27.0, 22.6, 21.0, 14.0.

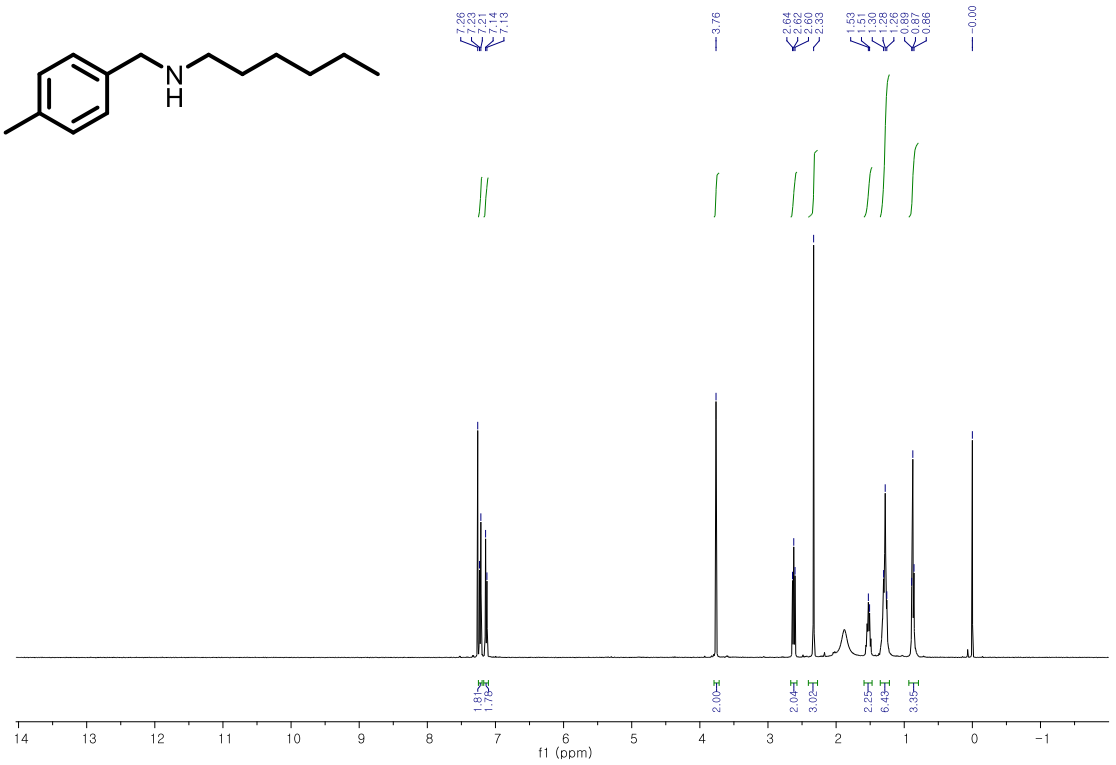

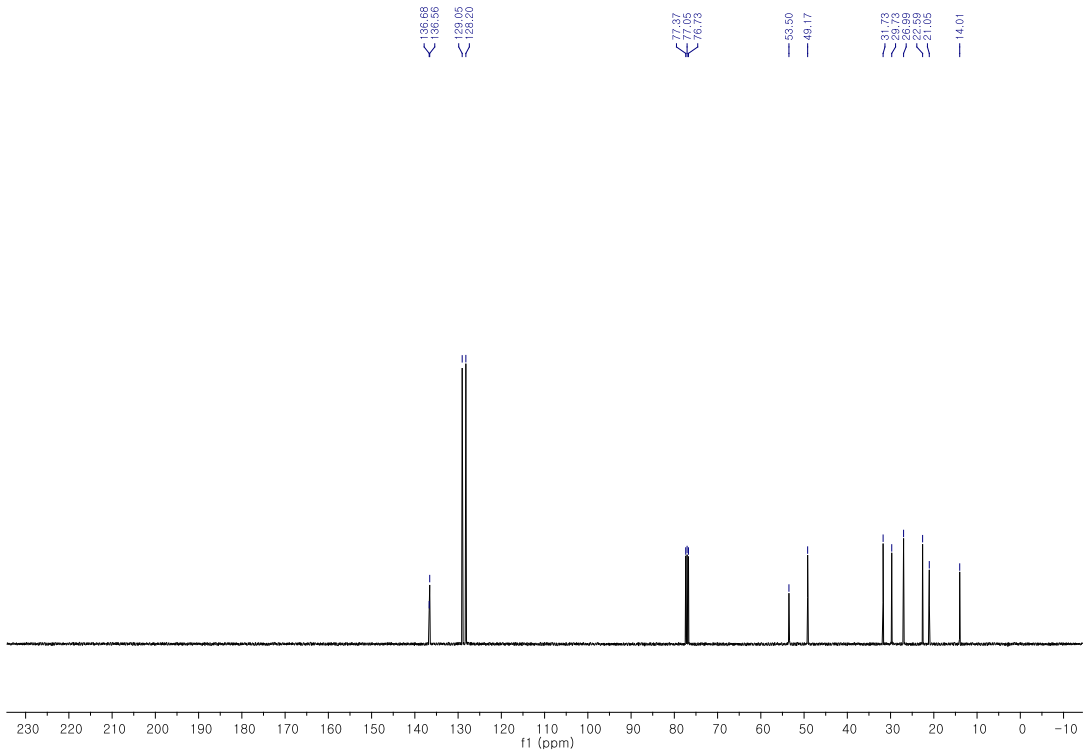

NMR S8, 3k, *N*-(4-(tert-butyl)benzyl)hexan-1-amine

60% (148mg, Colorless oil); ^{1}H NMR (400 MHz, $CDCl_3$) δ 7.36 (s, 1H), 7.34 (s, 1H), 7.27 (s, 1H), 7.25 (s, 1H), 3.76 (s, 2H), 2.64 (t, *J* = 7.3 Hz, 2H), 1.55 – 1.48 (m, 2H), 1.33 – 1.25 (m, 15H), 0.88 (t, *J* = 6.8 Hz, 3H).^{13}C NMR (101 MHz, $CDCl_3$) δ 149.8, 137.1, 127.9, 126.8, 125.4, 125.2, 53.6, 49.5, 34.4, 31.8, 31.3, 29.9, 27.0, 22.6, 14.0. HR-MS (EI): calcd for $C_{17}H_{29}N$ 247.2300; found: 247.2301.

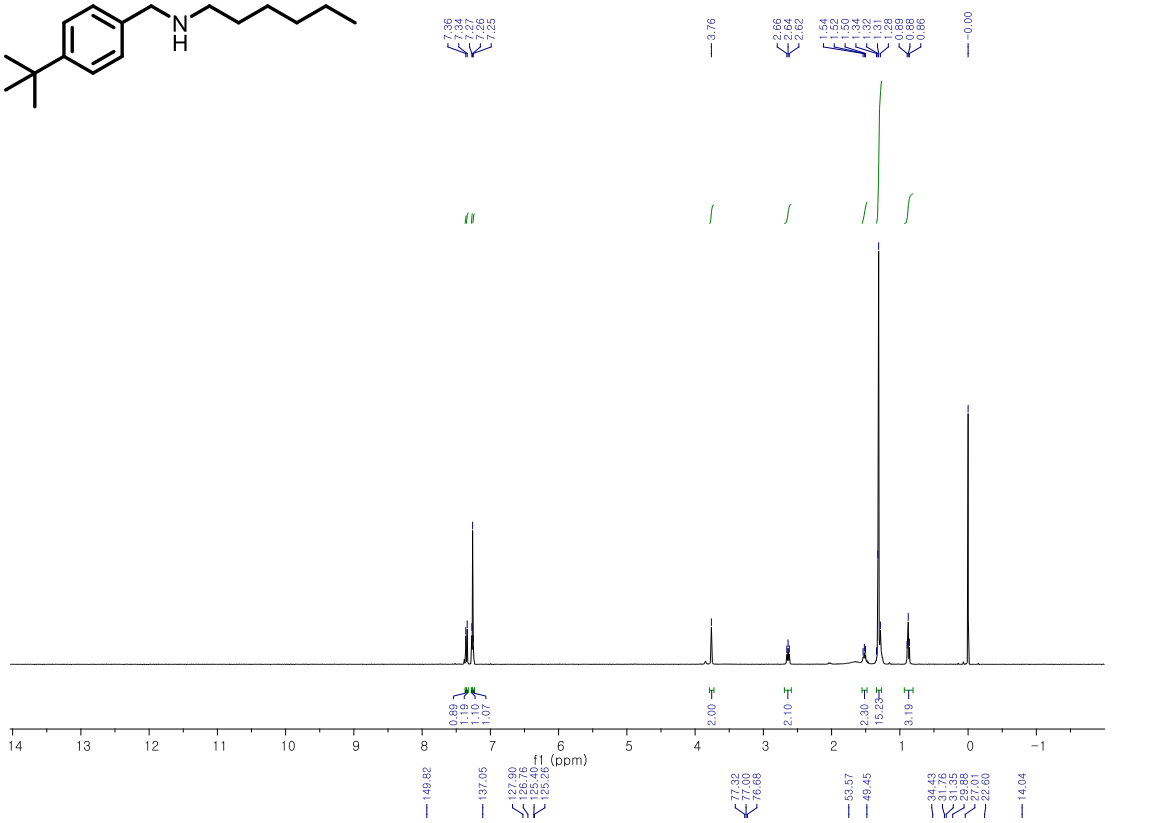

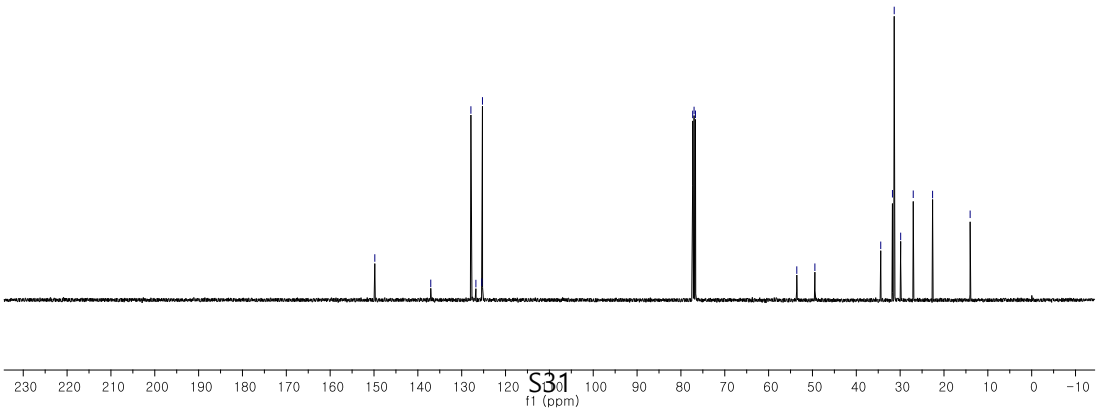

NMR S9, 3l, *N*-(2-fluorobenzyl)hexan-1-amine

62% (129.7 mg, Colorless oil) ;^{1}H NMR (400 MHz, $CDCl_3$) δ 7.33 (td, *J* = 7.6, 1.6 Hz, 1H), 7.25 – 7.19 (m, 1H), 7.10 (td, *J* = 7.5, 1.0 Hz, 1H), 7.07 – 6.99 (m, 1H), 3.84 (s, 2H), 2.61 (t, *J* = 7.2 Hz, 2H), 1.52-1.47 (m, 2H),1.33-1.26 (m, 6H) 0.88 (t, *J* = 6.8 Hz, 3H). ^{13}C NMR (101 MHz, $CDCl_3$) δ 161.18 (d, *J* = 245.2 Hz), 130.37 (d, *J* = 4.9 Hz), 128.56 (d, *J* = 8.2 Hz), 127.19 (d, *J* = 15.2 Hz), 123.98 (d, *J* = 3.5 Hz), 115.20 (d, *J* = 21.9 Hz), 49.27, 47.31. 31.73. 29.93, 26.97, 22.58, 14.01. HR-MS (EI): calcd for $C_{13}H_{20}FN$ 209.1580; found: 209.1579.

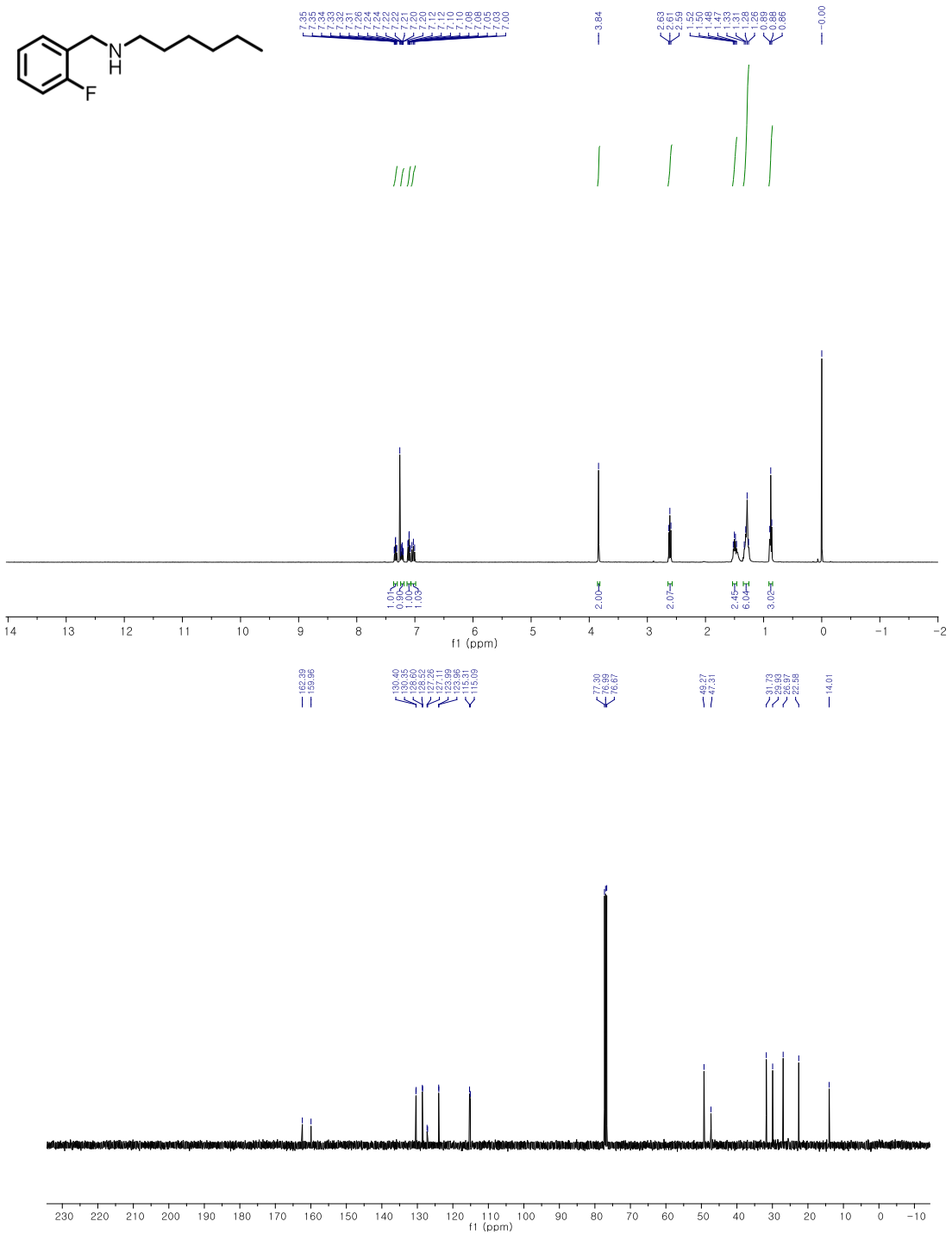

NMR S10, 3m, *N*-(3-fluorobenzyl)hexan-1-amine

60% (125 mg, Colorless oil); ^{1}H NMR (400 MHz, $CDCl_3$) δ 7.28 (t, *J* = 10.8 Hz, 1H), 7.07 (dd, *J* = 14.8, 8.6 Hz, 2H), 6.93 (td, *J* = 8.3, 2.0 Hz, 1H), 3.79 (s, 2H), 2.61 (t, *J* = 7.2 Hz, 2H), 1.57 – 1.42 (m, 2H), 1.37 – 1.24 (m, 6H), 0.88 (t, *J* = 6.7 Hz, 3H). ^{13}C NMR (101 MHz, $CDCl_3$) δ 162.93 (d, *J* = 245.6 Hz), 143.10 (d, *J* = 7.0 Hz), 129.71 (d, *J* = 8.2 Hz), 123.53 (d, *J* = 2.7 Hz), 114.81 (d, *J* = 21.2 Hz), 113.54 (d, *J* = 21.1 Hz), 53.39, 49.37, 31.72, 29.96, 26.97, 22.58, 13.99. HR-MS (EI): calcd for $C_{13}H_{20}FN$ 209.1580; found: 209.1582.

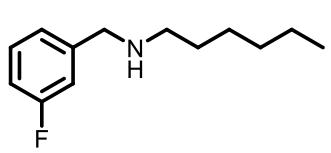

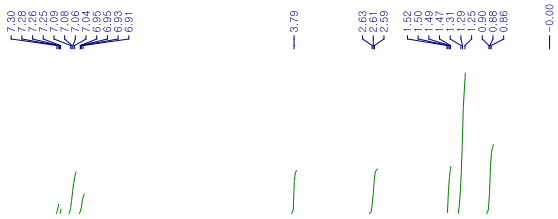

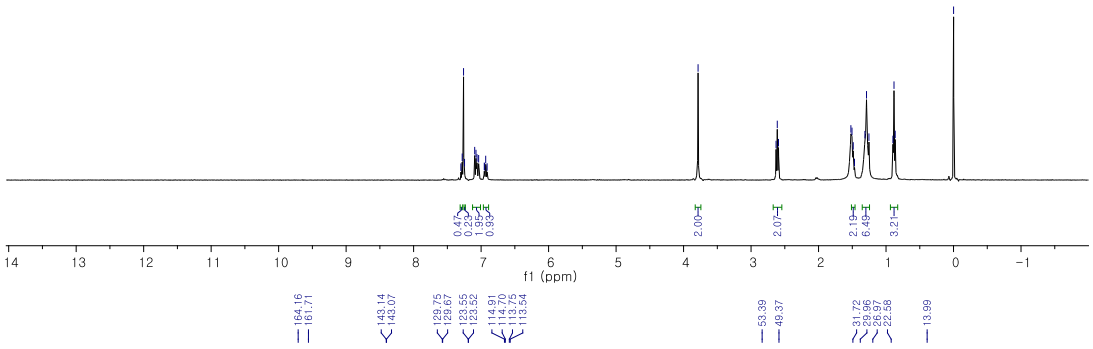

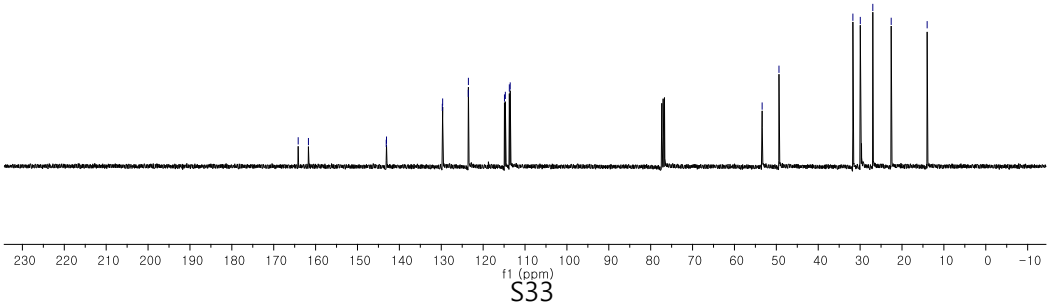

NMR S11, 3n, *N*-(4-fluorobenzyl)hexan-1-amine[15]

81% (169mg, Colorless oil) ; ^{1}H NMR (400 MHz, $CDCl_3$) δ 7.35 – 7.26 (m, 2H), 7.09 – 6.85 (m, 2H), 3.75 (s, 2H), 2.60 (t, *J* = 7.2 Hz, 2H), 1.54 – 1.44 (m, 2H), 1.37 – 1.19 (m, 6H), 0.88 (t, *J* = 6.7 Hz, 3H). ^{13}C NMR (101 MHz, $CDCl_3$) δ 161.82 (d, *J* = 244.5 Hz), 136.14 (d, *J* = 3.1 Hz), 129.57 (d, *J* = 7.9 Hz), 115.04 (d, *J* = 21.2 Hz), 53.25, 49.40, 31.74, 29.98, 27.00, 22.59, 14.00.

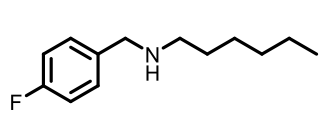

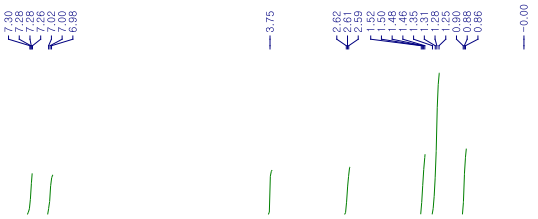

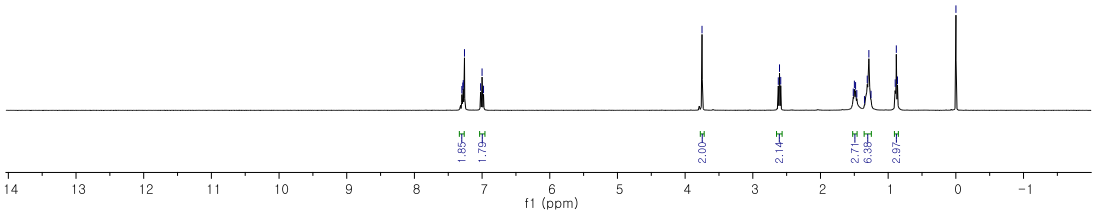

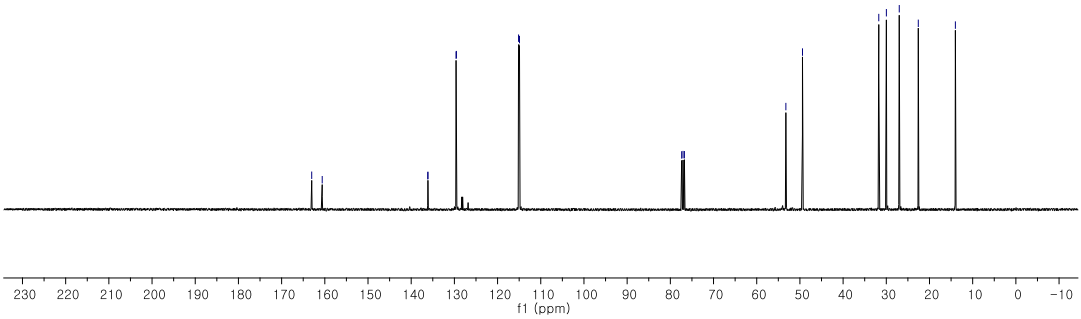

NMR S12, 3o, *N*-(naphthalen-2-ylmethyl)hexan-1-amine

87% (210mg, Yellow oil); ^{1}H NMR (400 MHz, $CDCl_3$) δ 7.82 (d, J = 8.3 Hz, 3H), 7.78 (s, 1H), 7.54 – 7.41 (m, 3H), 3.98 (s, 2H), 2.71 – 2.64 (m, 2H), 1.63 – 1.51 (m, 2H), 1.39 – 1.22 (m, 6H), 0.87 (t, J = 6.8 Hz, 3H).^{13}C NMR (101 MHz, $CDCl_3$) δ 138.07, 133.50, 132.67, 128.02, 127.71, 127.65, 126.62, 126.40, 125.95, 125.48, 54.18, 49.57, 31.84, 30.14, 27.10, 22.68, 14.11. HR-MS (EI): calcd for $C_{17}H_{23}N$ 241.1830; found: 241.1826.

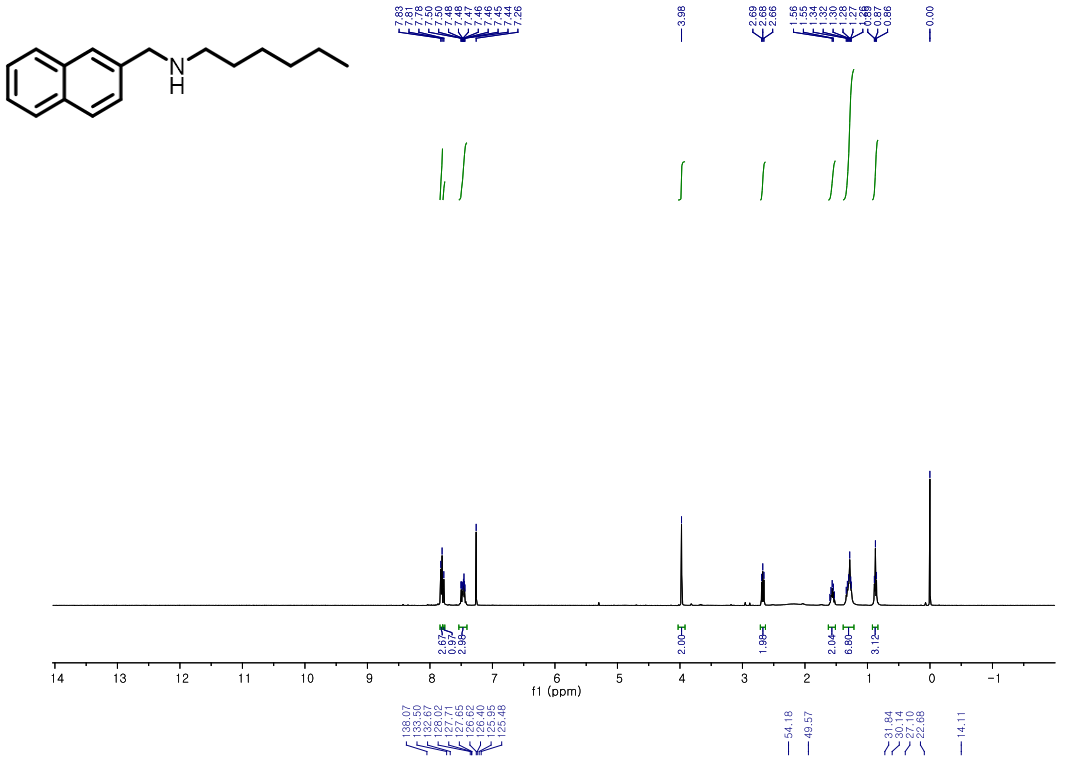

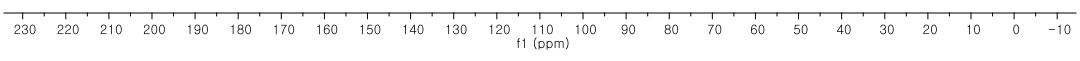

NMR S13, 3p, *N*-(4-methoxybenzyl)propan-1-amine[16]

80% (143 mg Colorless oil) ; ^{1}H NMR (400 MHz, $CDCl_3$) δ 7.26 (s, 1H), 7.24 (s, 1H), 6.87 (s, 1H), 6.85 (s, 1H), 3.80 (s, 3H), 3.73 (s, 2H), 2.59 (t, *J* = 7.3 Hz, 2H), 1.59 – 1.48 (m, 2H), 0.92 (t, *J* = 7.4 Hz, 3H). ^{13}C NMR(101 MHz, $CDCl_3$) δ159.7, 140.8, 129.4, 120.6, 113.7, 112.8, 55.2, 53.5, 50.8, 22.7, 11.7.

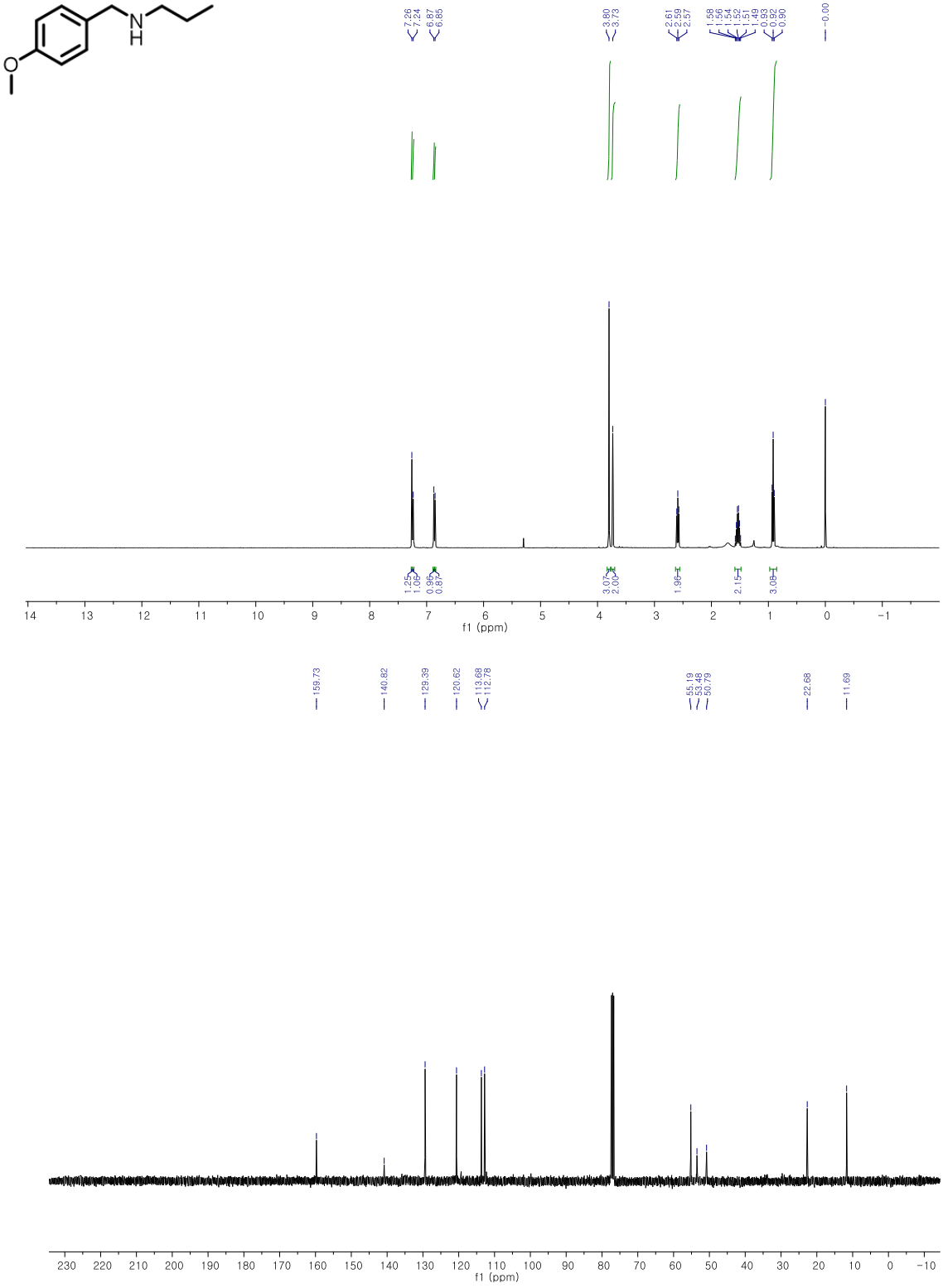

NMR S14, 3q, N-(4-methoxybenzyl)hexan-1-amine[9]

71% (157 mg, Colorless oil)**;** ^{1}H NMR (400 MHz, $CDCl_3$) δ 7.25 (s, 1H), 7.23 (s, 1H), 6.87 (s, 1H), 6.85 (s, 1H), 3.80 (s, 3H), 3.73 (s, 2H), 2.65 – 2.58 (m, 2H), 1.49 (dd, *J* = 14.7, 7.6 Hz, 2H), 1.28 (dd, *J* = 12.1, 6.5 Hz, 6H), 0.88 (t, *J* = 6.8 Hz, 3H). ^{13}C NMR (101 MHz, $CDCl_3$) δ 158.6, 132.1, 129.4, 113.7, 55.2, 53.3, 49.2, 31.7, 29.8, 27.0, 22.6, 14.0.

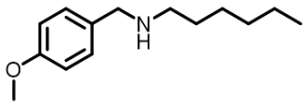

NMR S15, 3r, *N*-(3-methoxybenzyl)propan-1-amine[10]

66% (118mg ,Colorless oil); ^{1}H NMR (400 MHz, $CDCl_3$) δ 7.25 (s, 1H), 7.23 (s, 1H), 6.87 (s, 1H), 6.85 (s, 1H), 3.80 (s, 3H), 3.72 (s, 2H), 2.59 (t, *J* = 7.2 Hz, 2H), 1.53 – 1.47 (m, 2H), 0.91 (t, *J* = 7.4 Hz, 3H). ^{13}C NMR (101 MHz, $CDCl_3$) δ 159.7, 140.8, 129.4, 120.62, 113.7, 112.8, 55.2, 53.5, 50.8, 22.7, 11.7.

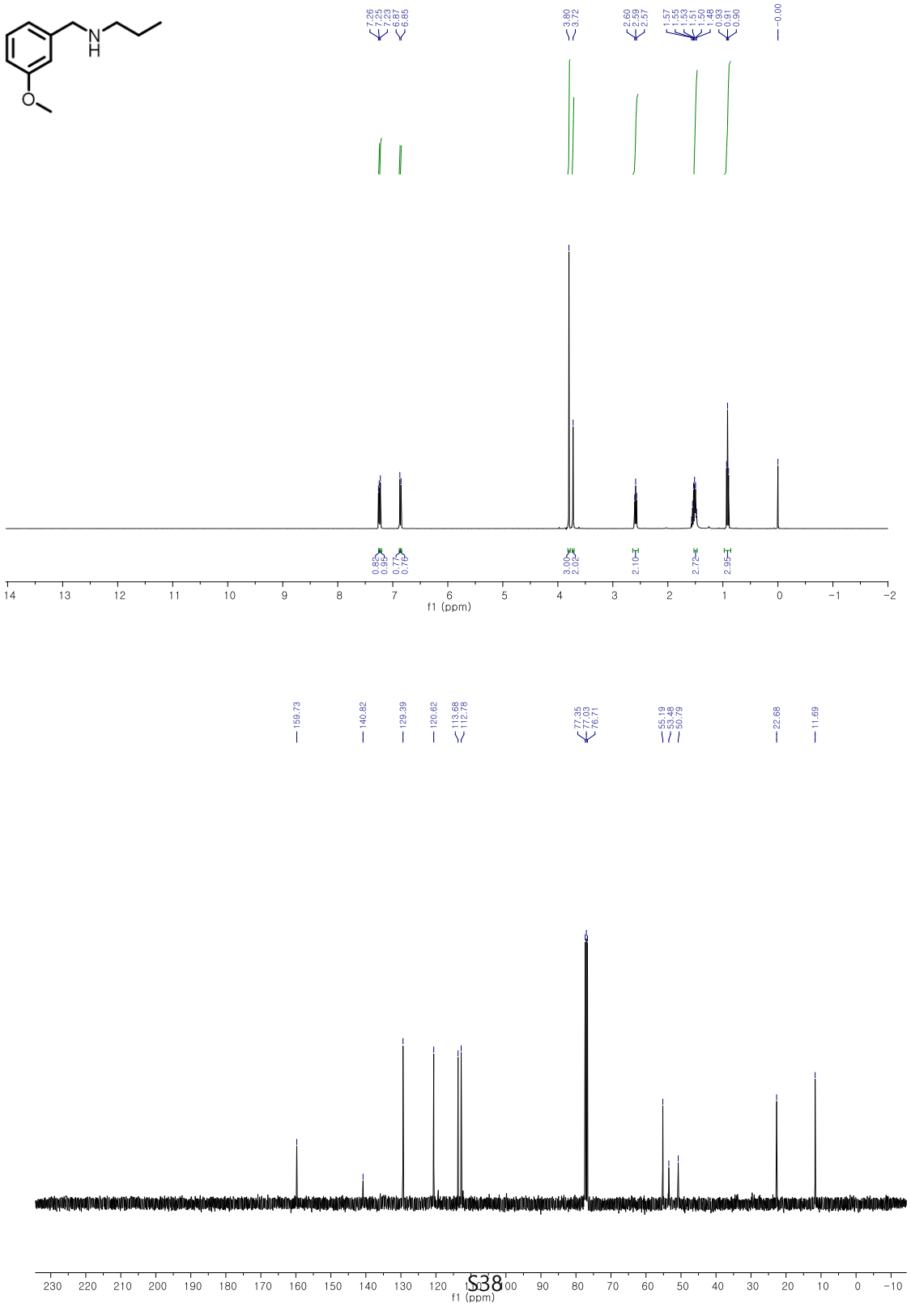

NMR S16, 3s, N-(3-methoxybenzyl)hexan-1-amine.

67% (148 mg, Yellow oil); ^{1}H NMR (400 MHz, $CDCl_3$) δ 7.23 (d, *J* = 7.7 Hz, 1H), 6.93 – 6.86 (m, 2H), 6.84 – 6.72 (m, 1H), 3.81 (s, 3H), 3.77 (s, 2H), 2.65 – 2.60 (m, 2H), 1.56 – 1.46 (m, 3H), 1.34 – 1.25 (m, 6H), 0.88 (t, *J* = 6.8 Hz, 3H). ^{13}C NMR (101 MHz, $CDCl_3$) δ 159.70, 142.04, 129.29, 120.39, 113.50, 112.39, 55.12, 53.95, 49.42, 31.77, 29.99, 27.02, 22.61, 14.03. HR-MS (EI): calcd for $C_{14}H_{23}NO$ 221.1780; found: 221.1781.

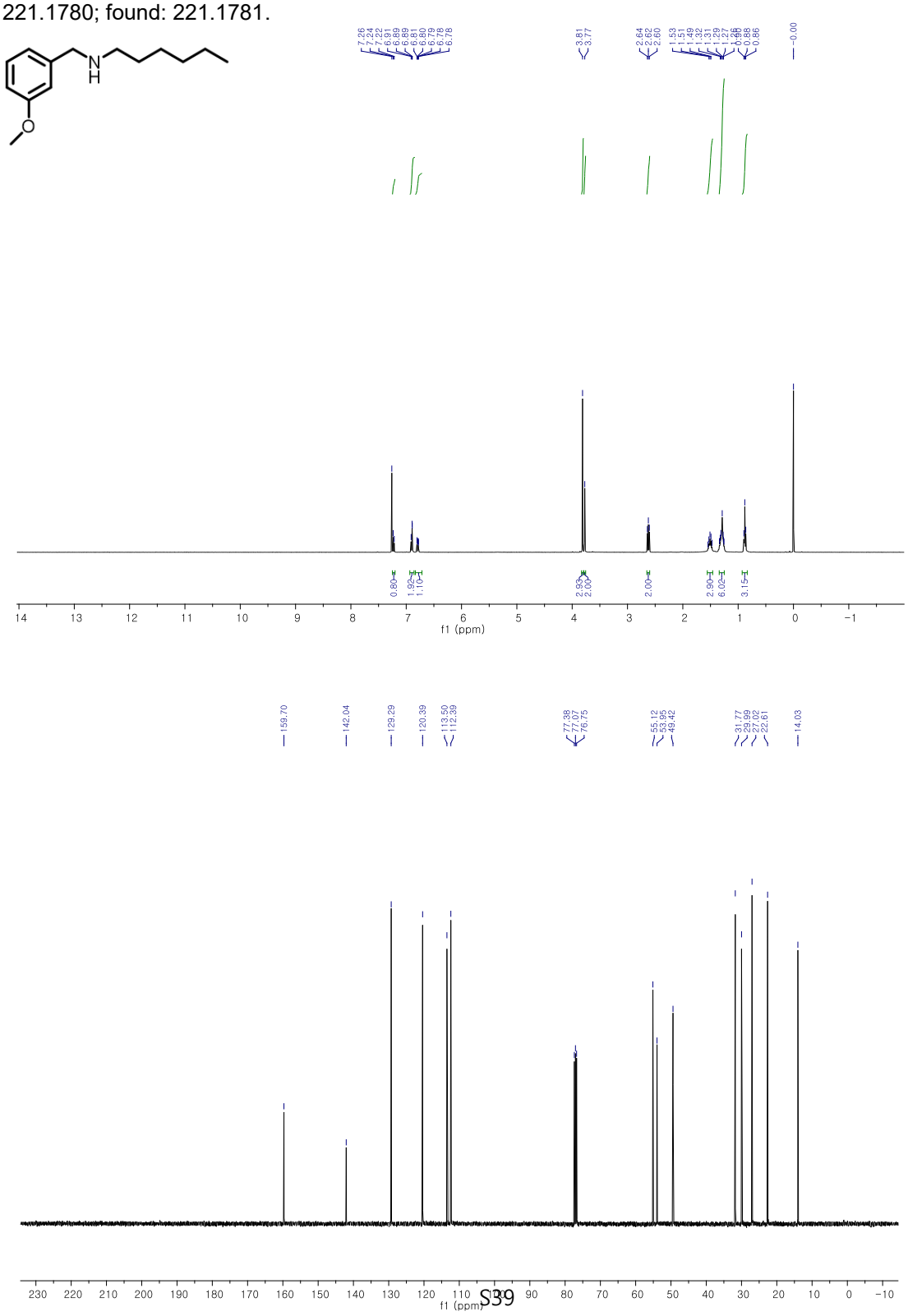

NMR S17, 3t, *N*-(4-ethoxybenzyl)hexan-1-amine.

73% (171 mg, Yellow oil); ^{1}H NMR (400 MHz, $CDCl_3$) δ 7.23 (s, 1H), 7.21 (s, 1H), 6.86 (s, 1H), 6.84 (s, 1H), 4.02 (q, *J* = 7.0 Hz, 2H), 3.72 (s, 2H), 2.64 – 2.55 (m, 2H), 1.53 – 1.45 (m, 2H), 1.40 (t, *J* = 7.0 Hz, 3H), 1.35 – 1.23 (m, 6H), 0.87 (d, *J* = 7.1 Hz, 3H). ^{13}C NMR (101 MHz, $CDCl_3$) δ 157.95, 132.06, 129.31, 114.29, 63.32, 53.32, 49.25, 31.74, 29.85, 27.01, 22.59, 14.81, 14.01. HR-MS (EI): calcd for $C_{14}H_{23}NO$ 235.1936; found: 235.1931.

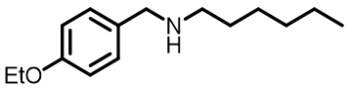

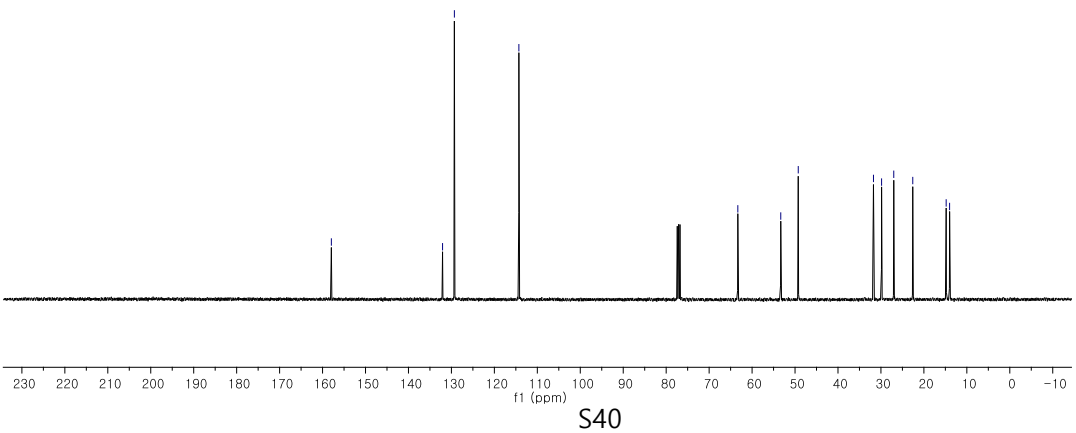

NMR S18, 3u, indole[17]

93% (117mg, White solid); ^{1}H NMR (400 MHz, $CDCl_3$) δ 7.65 (d, *J* = 7.9 Hz, 1H), 7.41 (dd, *J* = 8.1, 0.9 Hz, 1H), 7.22 (t, *J* = 2.8 Hz, 1H), 7.19 (dd, *J* = 8.1, 1.1 Hz, 1H), 7.15 – 7.09 (m, 1H), 6.57 (s, 1H). ^{13}C NMR (101 MHz, $CDCl_3$) δ 135.8, 127.8, 124.2, 121.9, 120.8, 119.83, 111.0, 102.6.

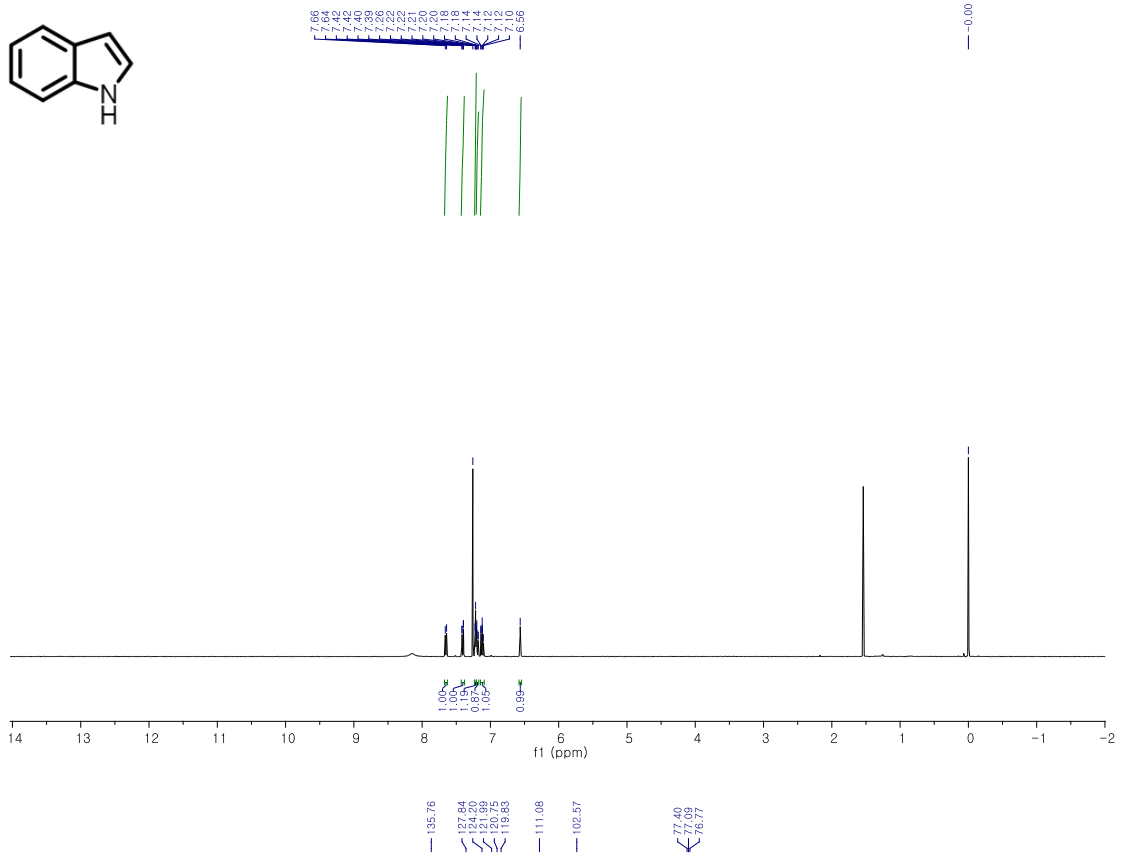

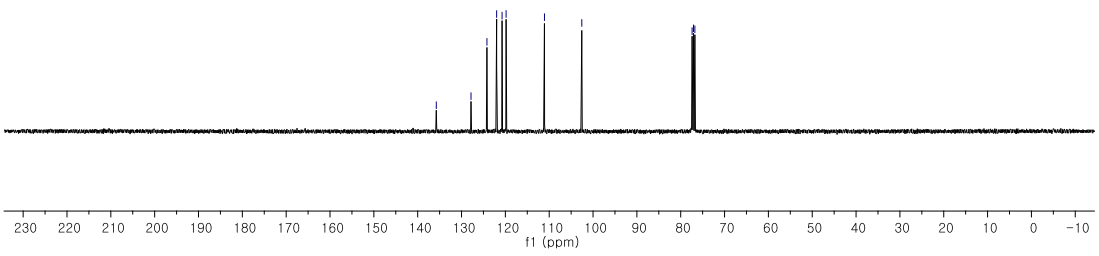

NMR S19, 5b, *N*-benzylcyclohexanamine[18]

64% (60mg, Yellow oil); ^{1}H NMR (400 MHz, $CDCl_3$) δ 7.35 – 7.26 (m, 5H), 3.80 (s, 2H), 2.49 (d, *J* = 3.6 Hz, 1H), 1.91 (d, *J* = 11.4 Hz, 2H), 1.78 – 1.69 (m, 2H),1.62-1.60 (br, 1H),1.29 – 1.06 (m, 5H). ^{13}C NMR (101 MHz, $CDCl_3$) δ 140.2, 128.4, 128.2, 126.9, 56.1, 50.8, 33.2, 26.1, 24.9.

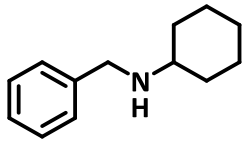

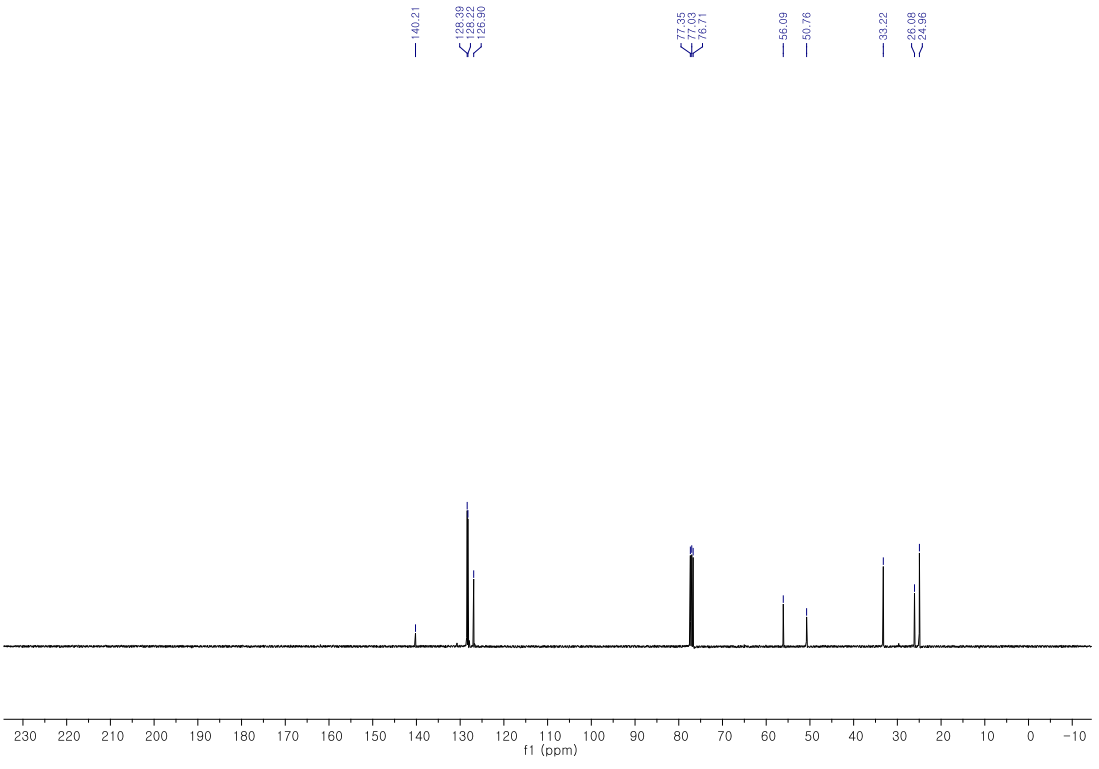

NMR S20, 5c, *N*-benzyl-4-methylbenzylamine[19]

81% (80 mg, Yellow oil); ^{1}H NMR (400 MHz, $CDCl_3$) δ 7.37 – 7.31 (m, 4H), 7.25-7.20 (m, 3H), 7.12 (d, J = 7.9 Hz, 2H), 3.81 (s, 2H), 3.78 (s, 2H), 2.35 (s, 3H).^{13}C NMR (101 MHz, $CDCl_3$) δ 140.4, 137.3, 136.5, 129.1, 128.4, 128.2, 128.1, 126.9, 53.1, 52.9, 21.1.

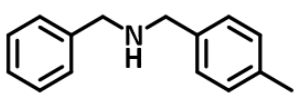

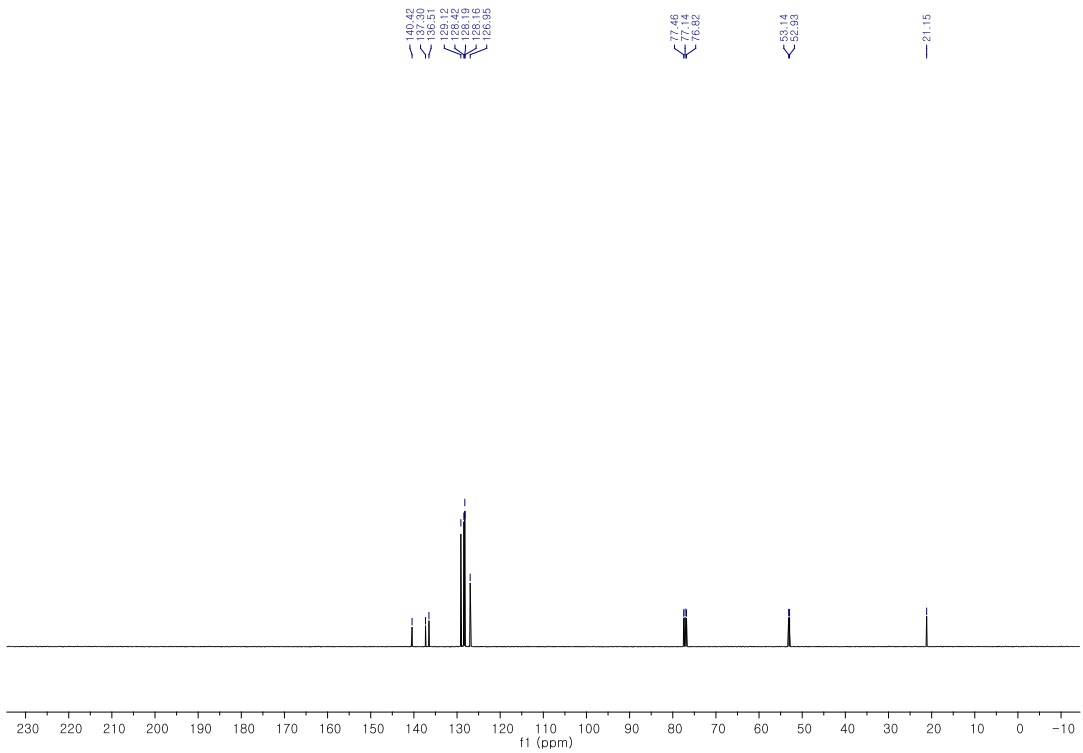

NMR S21, 5d, *N*-benzyl-1-(4-tert-butylbenzyl)amine[20]

78% (99mg Yellow oil); ^{1}H NMR (400 MHz, $CDCl_3$) δ 7.37-7.33 (m, 5H), 7.29-7.16 (m, 4H), 3.82 (s, 2H), 3.79 (s, 2H), 1.32 (s, 9H). ^{13}C NMR (101 MHz, $CDCl_3$) δ 149.9, 140.5, 137.4, 128.4, 128.2, 127.9, 127.9, 126.9, 125.3, 53.3, 52.9, 34.5, 31.5.

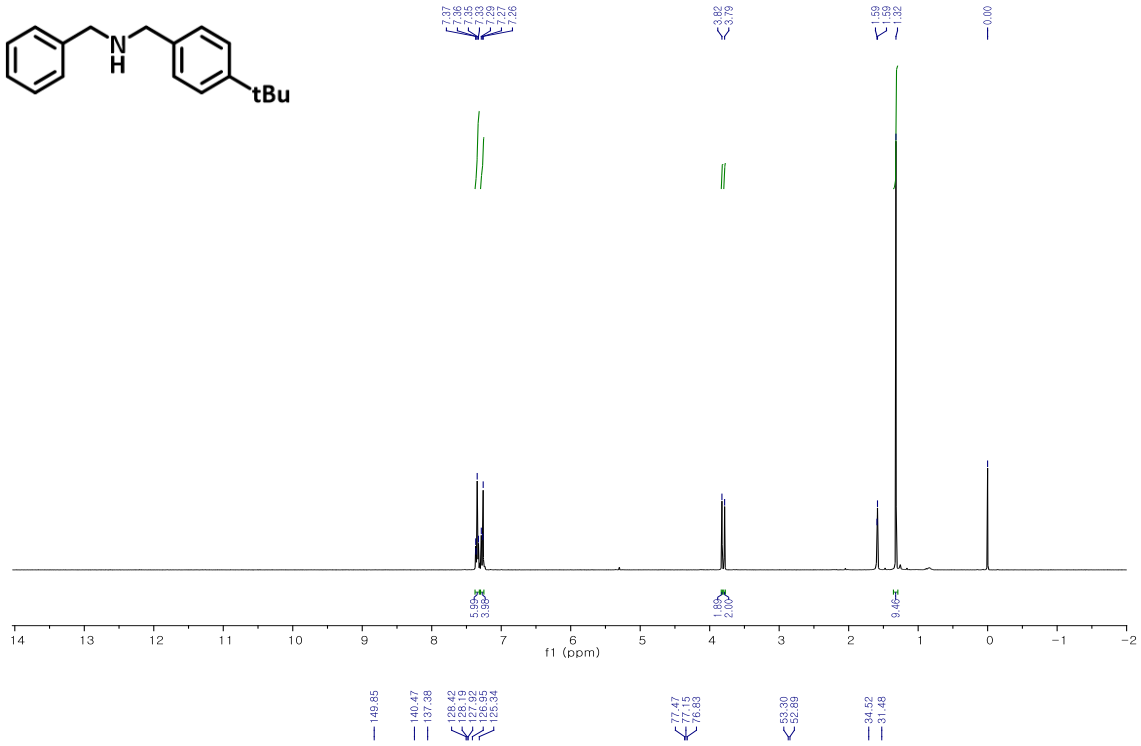

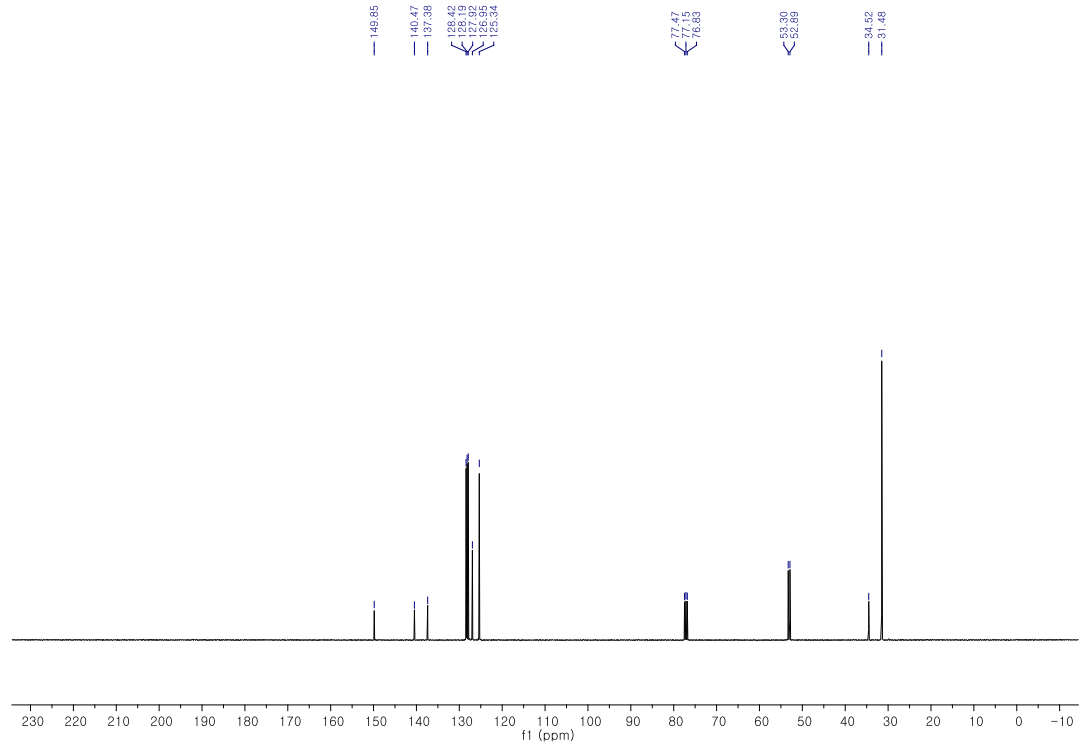

NMR S22, 5e, *N*-benzyl-1-(4-methoxyphenyl)methanamine[12]

92% (104 mg, Yellow oil); ^{1}H NMR (400 MHz, $CDCl_3$) δ 7.34 -7.22 (m, 7H), 6.87-6.86 (m, 2H), 3.83 – 3.72 (m, 7H). ^{13}C NMR (101 MHz, $CDCl_3$) 158.7, 140.2 123.3 129.4 128.4 128.2, 126.9, 113.8, 55.3, 53.0, 52.5.

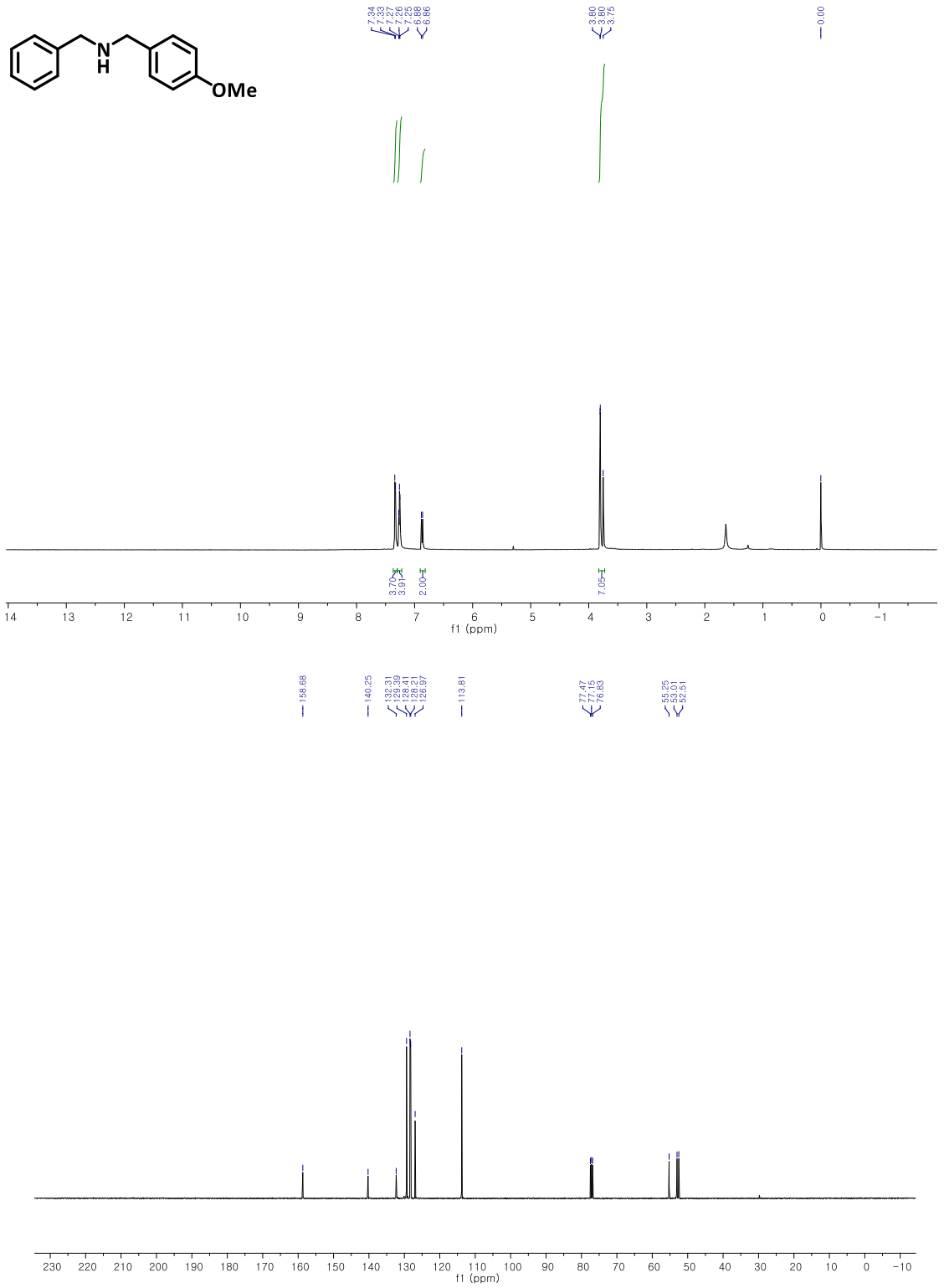

NMR S23, 5f, *N*-(4-methoxybenzyl)-1-(*p*-tolyl)methanamine[14]

81% (104mg, Colorless oil);^{1}H NMR (400 MHz, $CDCl_3$) δ 7.26 – 7.19 (m, 4H), 7.14 (d, *J* = 7.8 Hz, 2H), 6.87 (d, *J* = 8.6 Hz, 2H), 3.80 (s, 3H), 3.76 (s, 2H), 3.74 (s, 2H), 2.34 (s, 3H). ^{13}C NMR (101 MHz, $CDCl_3$) δ 158.6, 137.3, 136.5, 132.5, 129.3, 129.1, 128.15, 113.8, 55.23, 52.80, 52.51, 21.1.

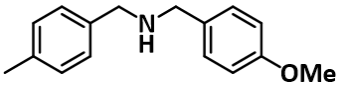

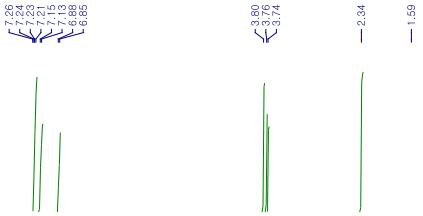

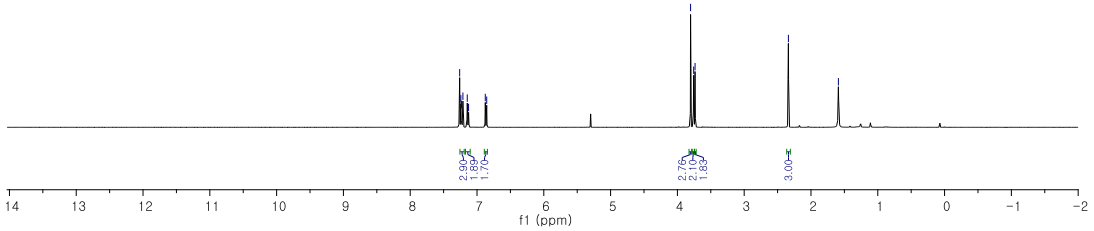

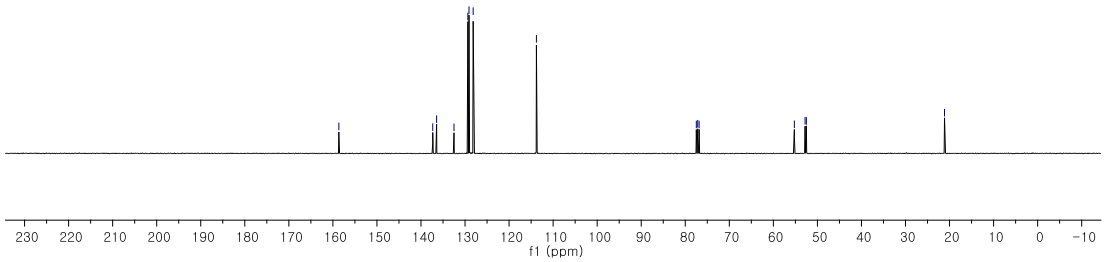

NMR S24, 5g, *N*-(4-fluorophenyl)methyl-1-(4-methoxyphenyl)methanamine[21]

81% (99 mg, Yellow oil); ^{1}H NMR (400 MHz, $CDCl_3$) δ 7.30 (dd, *J* = 8.5, 5.6 Hz, 2H), 7.24 (m, 2H), 7.01 (t, *J* = 8.7 Hz, 2H), 6.87 (d, *J* = 8.6 Hz, 2H), 3.80 (s, 3H), 3.76 (s, 2H), 3.73 (s, 2H). ^{13}C NMR (101 MHz, $CDCl_3$) δ 161.88 (d, *J* = 244.4 Hz), 158.66, 135.93, 132.18, 129.64 (d, *J* = 7.9 Hz), 129.30, 115.10 (d, *J* = 21.2 Hz), 113.79, 55.23, 52.45, 52.22.

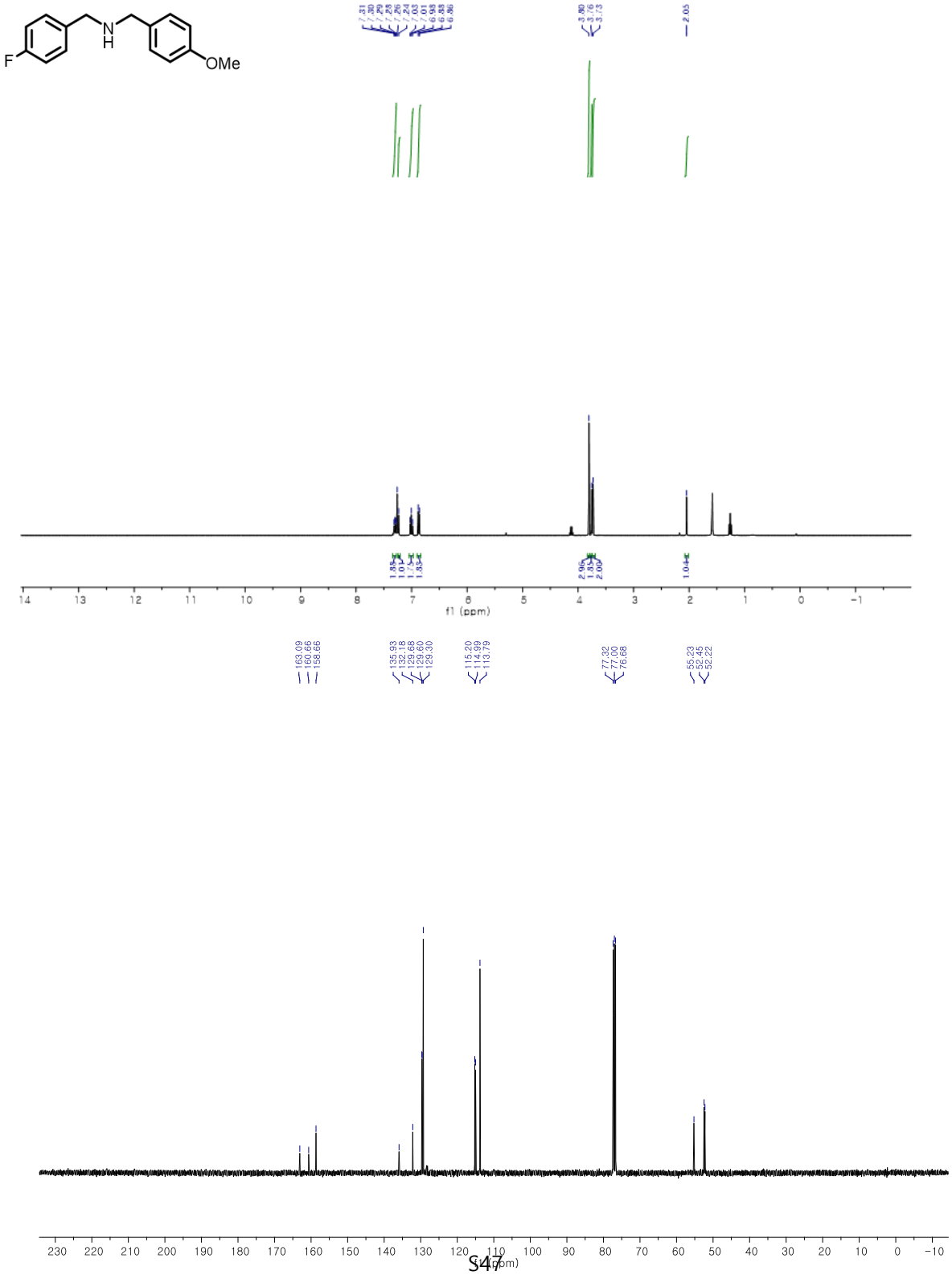

5. Reference

[1] A. Galan, J. de Medoza, P. Prados, J. Rojo, A. M. Echavarren, *J. Org. Chem*. 1991, **56***,* 452.

[2] S. Lu, J. Wang, X. Cao, X. Li, H. Gu, *Chem. Commun.* 2014, **50***,* 3512-3515.

[3] L. Liu, Y. Liu, Y. Ai, J. Li, J. Zhou, Z. Fan, H. Bao, R. Jiang, Z. Hu, J. Wang, K. Jing, Y. Wang, Q. Liang, H. Sun, *iScience* 2018, **8**, 61-73.

[4] Y. Li, Y. Gong, X. Xu, P. Zhang, H. Li, Y. Wang, *Catal. Commun.* 2012, **28***, 9-12.*

[5] S. Lu, P. Xu, X. Cao, H. Gu, *RSC Adv.* 2018, **8***,* 8755-8760.

[6] Z.-F. Jiao, J.-X. Zhao, X.-N. Guo, X.-L. Tong, B. Zhang, G.-Q. Jin, Y. Qin, X.-Y. Guo, *Catal. Sci. & Technol.* 2019, **9***,* 2266-2272.

[7] T. Ikawa, Y. Fujita, T. Mizusaki, S. Betsuin, H. Takamatsu, T. Maegawa, Y. Monguchi, H. Sajiki, *Org. Biomol. Chem.* 2012, **10**, 293-304

[8] S. K. Sharma, J. Lynch, A. M. Sobolewska, P. Plucinski, R. J. Watson, J. M. J. Williams, *Catal. Sci. Technol.* 2013, **3**, 85-88.

[9] Wetzel, S. Wockel, M. Schelwies, M. K. Brinks, F. Rominger, P. Hofmann and M. Limbach, *Org. Lett.* 2013*,* **15***,* 266-269*.*

[10] K. Orito, A. Horibata, T. Nakamura, H. Ushito, H. Nagasaki, M. Yuguchi, S. Yamashita and M. Tokuda, *J. Am. Chem. Soc.,* 2004*,* **126***,* 14342-14343*.*

[11] F. Mao, D. Sui, Z. Qi, H. Fan, R. Chen and J. Huang, *RSC Adv.* 2016*,* **6***,* 94068-94073.

[12] Z. Shao, S. Fu, M. Wei, S. Zhou and Q. Liu, *Angew. Chem. Int. Ed.* 2016**, 55***,* 14653-14657.

[13] W. Zhang, X. Dong and W. Zhao, *Org. Lett.* 2011*,* **13***,* 5386-5389*.*

[14] H. Chung and Y. K. Chung, *J. Org. Chem.* 2018, **83***,* 8533-8542.

[15] P. T. K. Arachchige, H. Lee and C. S. Yi, *J.Org. Chem.* 2018*,* **83***,* 4932-4947*.*

[16] O. Saidi, A. J. Blacker, M. M. Farah, S. P. Marsden and J. M. Williams, *Chem. Commun.* 2010**, 46***,* 1541-1543.

[17] Y. Motoyama, K. Kamo and H. Nagashima, *Org. Lett.* 2009*,* **11***,* 1345-1348.

[18] D. Wei, A. Bruneau-Voisine, D. A. Valyaev, N. Lugan and J. B. Sortais, *Chem. Commun.,* 2018*,* **54***,* 4302-4305.

[19] O. Y. Lee, K. L. Law and D. Yang, *Org. Lett,* 2009*,* **11***,* 3302-3305.

[20] S. Das, B. Join, K. Junge and M. Beller*, Chem. Commun,* 2012**, 48***,* 2683-2685*.*

[21] C. J. Smith, C. D. Smith, N. Nikbin, S. V. Ley and I. R. Baxendale, *Org. Biomol. Chem.* **2011,** *9,* 1927-1937.